THE ASTROPHYSICAL JOURNAL, 412:568–585, 1993 August 1

THE X-RAY STRUCTURE AND SPECTRUM OF NGC 6251

M. BIRKINSHAW AND D. M. WORRALL
Harvard-Smithsonian Center for Astrophysics, 60 Garden Street, Cambridge, MA 02138
Received 1992 November 9; accepted 1993 February 8

ABSTRACT

NGC 6251 has been observed in low-energy X-rays with the Position Sensitive Proportional Counter on board *ROSAT*. No X-ray emission is seen from the 4'.5 long radio jet of this galaxy, suggesting that the electron spectrum is cut off for electron energies greater than $E_{max} \approx 10^{12}$ eV, but a bright X-ray source is coincident with the center of the galaxy. Most of the counts in this source are in a component of small angular size, FWHM $< 4''$, corresponding to a linear size less than 3 kpc, although there is evidence for the presence of a low surface brightness halo with FWHM $\sim 3'$. If this halo is thermal bremsstrahlung of gas near NGC 6251, this gas cannot confine the arcminute-scale radio jet by simple (static) gas pressure.

The spectrum of the X-ray core source in NGC 6251 is a bad match to a single-component thermal model and, when fitted by a simple power-law model, requires the presence of an absorbing column far in excess of the Galactic or intrinsic columns. The nuclear spectrum can be well fitted by a composite model with two (or more) different components: a plausible decomposition consists of a flat-spectrum (energy index $\alpha_X \approx 0.27$) power-law component from a mini–active galactic nucleus (AGN) plus an 0.5 keV thermal component. The power-law spectral index is close to the high-frequency radio spectral index of the VLBI core, supporting a synchro–self-Compton model for this component of the X-ray emission. The temperature of the thermal component is characteristic of the temperatures of gas found in other elliptical galaxies, and the gas must be in a cooling flow. The infall of material into the nucleus is sufficiently rapid to power the mini–AGN component, if the mass of the central black hole exceeds $5 \times 10^4\ M_\odot$. Unification schemes that relate BL Lac objects and radio galaxies (e.g., Padovani & Urry 1990) require a component of unbeamed X-ray emission: it is possible that the type of thermal gas that we find in NGC 6251 may produce the necessary unbeamed X-ray component.

Subject headings: galaxies: individual (NGC 6251) — galaxies: jets — galaxies: nuclei — radiation mechanisms: miscellaneous — X-rays: galaxies

1. INTRODUCTION

The magnetic fields and particle beams that underlie the jets of low-luminosity radio galaxies may be confined by the pressure of the galaxy or cluster atmosphere in which they are embedded (e.g., Henriksen, Vallée, & Bridle 1981), although stronger, dynamical, interactions such as ram pressure are needed to explain the morphologies of distorted sources such as NGC 1265 (Begelman, Blandford, & Rees 1980) or 3C 465 (Leahy 1984). The details of both types of interaction depend on the nature of the beam and the structure of the atmosphere through which it propagates, but for laminar, turbulent, and magnetic field–dominated flows it appears that pressure-confined beams propagating in simple stratified atmospheres will adopt structures similar to those seen in some radio sources (Henriken, Vallée, & Bridle 1981; Henriksen, Bridle, & Chan 1982; Hardee et al. 1992).

Some direct tests of these ideas have been made (e.g., for M87, where it appears that the jet is overpressured relative to the galaxy atmosphere; Owen, Hardee, & Cornwell 1989), but this has been difficult because of the small number of cases where both the radio and the gas structures are well mapped. For a radio jet in a cluster of galaxies, the unknown three-dimensional distance of the jet from the cluster center makes it difficult to establish the pressure and density environment through which the galaxy moves. For example, NGC 1265 is known to be in rapid motion relative to the center of the Perseus Cluster, but its unknown distance from the cluster center prevents the sure knowledge that the density of the surrounding gas is sufficient for ram pressure to bend the jets.

The best case for the study of the interaction of a jet with the external medium would be provided by a large angular size jet associated with a relatively isolated and nearby galaxy. Then the variation of density with distance down the jet can be more easily determined (although the projection of the jet relative to the line of sight may still be unknown), and there should be no significant motion of the atmosphere over most of the jet. The radio source associated with NGC 6251 (Waggett, Warner, & Baldwin 1977) is one of the brightest and most extended examples of a radio jet associated with a nearby, isolated elliptical galaxy, and represents one of the best opportunities to study jet propagation. We have therefore observed NGC 6251 with the *ROSAT* Position Sensitive Proportional Counter (PSPC; Trümper 1983; Pfefferman et al. 1987; Aschenbach 1991; Trümper 1992) to obtain images with moderate ($\sim 25''$ FWHM) angular resolution and useful spectral resolution with the purpose of studying the ambient medium around the galaxy and its radio jet.

NGC 6251 is a 13.5 mag E2 galaxy which shows some evidence for cold gas and dust (Nieto et al. 1983) but has no detectable neutral hydrogen in absorption against its radio nucleus (van Gorkom et al. 1989). The heliocentric velocity of the galaxy is 7400 km s^{-1} (J. Huchra 1991, private communication), corresponding to a distance ≈ 150 Mpc (for $H_0 = 50$ km s^{-1} Mpc^{-1} and $q_0 = 0.1$). NGC 6252 (of

unknown redshift) lies a few arcminutes to the north of NGC 6251, and both galaxies are said to lie in the outer parts of Zwicky cluster Zw 1609.0+8212 (Young et al. 1979). However, the velocity separation between NGC 6251 and the mean velocity of this (small) cluster is ≈ 1000 km s^{-1}, so that it is likely that the cluster is not a strong influence on NGC 6251. Prestage & Peacock (1988) found that the local density of galaxies near NGC 6251 is low, so that the only gas near the jet is likely to be the atmosphere of NGC 6251 itself, rather than a hotter gas associated with a cluster.

NGC 6251 became of wide interest when it was found to be the parent galaxy of an exceptional radio jet (Waggett et al. 1977). The gross structure of the radio source is that of a large ($\sim 1°$) asymmetric double, with the brighter northwest radio lobe (Willis et al. 1982) fed by a 4'.5 long radio jet which has been well mapped by Perley, Bridle, & Willis (1984a); they used the morphology of the jet to infer that it is confined (perhaps by the atmosphere of NGC 6251) at angles $\gtrsim 20''$ from the nucleus but unconfined on smaller scales. VLBI observations of the bright radio core of the galaxy reveal a parsec-scale jet which is one-sided in the same sense as the kiloparsec-scale jet, but slightly misaligned relative to it (Cohen & Readhead 1979; Jones et al. 1986) in the sense that the jet bends toward the minor axis of the galaxy by 6° between the parsec and kiloparsec scales.

Since Keel (1988) has detected optical emision from the jet region $\approx 20''$ from the core, it might also be possible to detect the jet in the X-ray wave band: if the X-ray–to–radio ratio of the NGC 6251 jet were similar to that of the M87 jet (Biretta, Stern, & Harris 1991), then it would be easily detected with the *ROSAT* PSPC. However, Keel's data show that the optical continuum of the NGC 6251 jet is very steep, and an extrapolation into the X-ray from the optical spectrum alone would suggest that the jet would be undetectable.

X-ray data from the *Einstein* Imaging Proportional Counter (IPC) indicate a luminosity for NGC 6251 of $\approx 1.4 \times 10^{35}$ W in the 0.2–3.5 keV band (Jones et al. 1986), but the resolution of the IPC was insufficient to show whether this emission is produced by a source at the center of the galaxy, the jet, or a galactic atmosphere with gas mass $\sim 2 \times 10^{10}\ M_\odot$ (scaling from the galaxies studied by Forman, Jones, & Tucker 1985). If the X-ray emission is produced by the galaxy atmosphere, then Perley et al. (1984a) estimated that it could provide the confinement of the outer radio jet that they infer from their radio map.

Our observation with the *ROSAT* PSPC was planned to detect this possible galaxy atmosphere to the edge of the jet, and to use the X-ray surface brightness profile and spectrum to obtain good estimates of the confining pressure around the jet. This would establish whether this jet is confined by the galactic atmosphere, and whether the changing character of the jet with distance from the core is associated with structure in the galactic atmosphere. In § 2 we describe the X-ray data obtained with the *ROSAT* PSPC. No detectable X-radiation was found associated with the jet: these results and their implications are discussed in § 3. Section 4 then considers in detail the angular structure of the X-ray source associated with NGC 6251 and uses the surface brightness profile to show that the atmosphere of the galaxy cannot provide sufficient pressure to confine the radio jet. In § 5 we discuss the spectrum of the nuclear X-ray emission, and show that the X-ray source plausibly consists of thermal and nonthermal components with comparable soft X-ray luminosity. The overall conclusions are summarized in § 6, which also interprets the results in terms of a composite model for the source consistent with unified schemes for active galactic nuclei (AGNs).

2. THE X-RAY DATA

We observed NGC 6251 in soft X-rays with the *ROSAT* PSPC (Trümper 1983; Pfefferman et al. 1987; Aschenbach 1991; Trümper 1992) as the target of a pointing during the AO 1 phase of the mission. A total of 14,830 s of live observing time on source were accumulated in seven periods between 1991 March 13 and March 16. The boron filter was not used in front of the PSPC so that the maximum possible efficiency for the detection of X-rays from NGC 6251 would be obtained.

The observations were made with the (~ 400 s) wobble of the spacecraft relative to the target direction turned on. This wobble averages over occultations of X-ray sources by the wire support structure of the PSPC window, avoiding the potential loss of weak features behind individual wires. The arrival positions of the photons were corrected for this wobble, and other instrumental effects, by the Standard Analysis Software System (SASS; Gruber 1992). Results in this paper are based on SASS version 5_2 having been applied to the data. SASS performs a preliminary analysis of the data. We used the Post Reduction Off-Line Software (PROS; Worrall et al. 1992) in the IRAF environment (Tody 1986) to perform the additional analysis required for this work.

The X-ray detection of NGC 6251 in these data has good signal-to-noise ratio, with 1521 ± 44 net counts (0.1–2.4 keV), using an on-source circle of 2' radius and local background from an annulus of radii 2' and 4'. The centroid of the X-ray emission as determined by SASS is roughly 8" to the north and 4" to the west of the radio core (which is at R.A. $16^h32^m32^s.013$, decl. 82°32'16".40 (J2000), with an error $\pm 0''.10$; NRAO 1990). Since this offset is within *ROSAT*'s absolute positional uncertainty ($\sim 10''$, and currently under investigation; Max-Planck-Institut für Extraterrestrische Physik, Newsletter No. 10, 1992 August), and since it is not in a direction related to the radio morphology, we interpret the X-ray emission as coming from the radio core, and we have shifted the X-ray data accordingly. Figure 1 is a contour plot of 330 MHz VLA radio data (Birkinshaw et al. 1993) superposed on the shifted X-ray image. Our result for angular structure is that the X-ray emission is roughly consistent with a point source, with the photons spread only by the PSPC on-axis point response of about 25" FWHM (Hasinger et al. 1992). The lack of extended X-ray emission associated with the radio jet is discussed in § 3 below, and detailed fits to the angular structure of the X-ray source are presented in § 4, while an analysis of the spectrum of the emission is given in § 5.

3. THE KILOPARSEC-SCALE JET OF NGC 6251

The arcsecond-to-arcminute radio jet of NGC 6251 lies between (J2000) position angles 291°.6 and 299°.0, where the opening angle of 7°.4 takes account of both the broadening of the radio jet and its slight side-to-side deviations from a linear flow. We can assess the X-ray brightness of the jet in some range of radii by comparing the counts in this segment of the image with the counts in the remaining sectors of similar annuli about the center of the galaxy. This procedure requires that the X-ray emission from the galaxy be circularly symmetric, an assumption that is validated by the similarity of the radial profiles of the source extracted in different quadrants about the source centroid (§ 4).

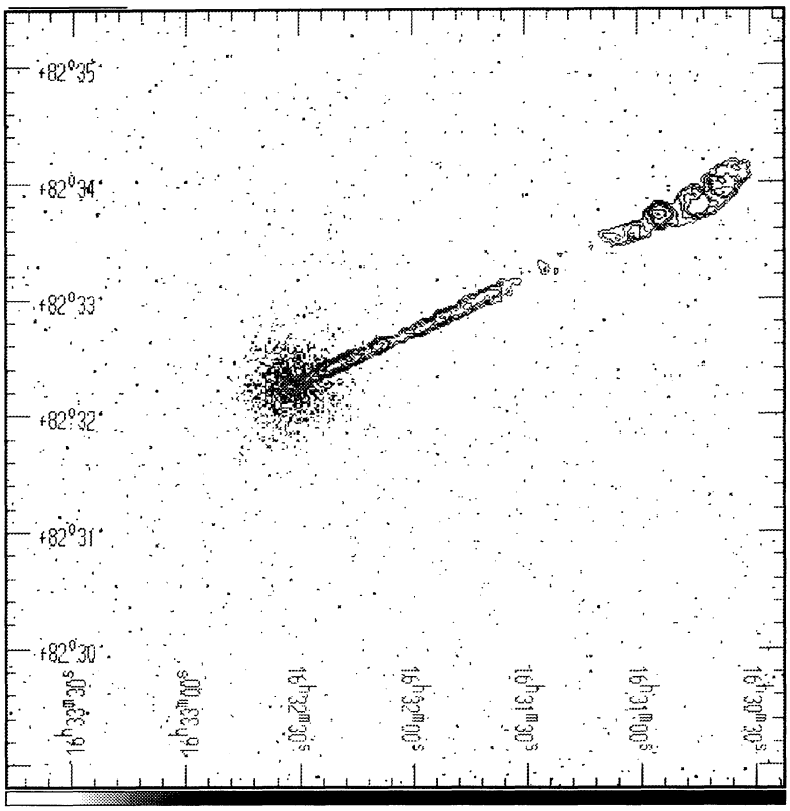

FIG. 1.—Contour plot of a 330 MHz radio map of NGC 6251 (Birkinshaw et al. 1993) superposed on the *ROSAT* PSPC 0.2–2.4 keV X-ray image after shifting the location of the centroid of the X-ray emission to coincide with the location of the compact central component of the radio source (see text). The coordinate grid is J2000. Note that the X-ray emission is well confined to a small region around the core of the radio source (and the nucleus of the elliptical galaxy) and that there is no evidence for excess X-radiation associated with the radio jet.

It is most useful to extract these surface brightness limits over the ranges of radius which correspond to coherent and well-defined features in the radio image. Four such jet features are apparent on the radio map (Fig. 1). Ignoring the emission from the central source for the present, they will be denoted features A, B, C, and D, where A is the brightest part of the jet, which lies 10″–40″ from the nucleus; B is the "knotty" region from 40″ to 126″ from the nucleus; C is the low-brightness region from 126″ to 178″ from the nucleus; and D is the high-brightness outer part of the jet, from 178″ to 264″ from the nucleus, after which the jet bends significantly to the north (see Fig. 1).

The count-rate excesses in the X-ray emission from these jet regions, relative to other sectors of annuli about the nucleus, are given in Table 1 in terms of both the PSPC count rate and the 1 keV flux density, derived on the assumptions that the X-ray spectrum of the jet is a power law of energy index $\alpha_X = 1$, and that the neutral hydrogen column density toward the jet is given by its Galactic value ($N_H = 5.5 \times 10^{20}$ atoms cm^{-2}; Stark et al. 1992) so that 1 count s^{-1} (in 0.1–2.4 keV) $\approx$ 3.37 μJy. For values of α_X in the range $0 < \alpha_X < 2$, this conversion factor between the count rate and the 1 keV flux density varies by less than 30%, so that the choice $\alpha_X = 1$ is unlikely to produce a qualitative error in our interpretation of the results. The error estimates in Table 1 have been checked by performing the same analysis in 35 other 7°.4 ranges of position angle, offset by 10°, 20°, ..., 350° from the radio jet. The scatter of the results at these different position angles is roughly consistent with the noise estimates in Table 1. Since none of the values in the table indicates a detection of the jet, we adopt 3 σ upper limits of 2, 2, 2, and 5 nJy for the flux densities of features A, B, C, and D, respectively.

TABLE 1

X-RAY SURFACE BRIGHTNESS OF THE JET

Feature	Radius (arcsec)	Area (arcmin^2)	Count Rate (counts s^{-1} arcmin^{-2})	1 keV Flux Density (nJy)
A	10–40	0.027	-0.0347 ± 0.0071	-3.1 ± 0.6
B.....	40–126	0.26	-0.00022 ± 0.00078	-0.2 ± 0.6
C	126–178	0.28	-0.00059 ± 0.00056	-0.6 ± 0.5
D	178–264	0.68	0.00085 ± 0.00050	2.0 ± 1.1

NOTE.—The 1 keV flux densities are calculated on the assumption that the X-ray spectrum is a power law of energy index $\alpha_X = 1$ which has been absorbed by gas equivalent to the Galactic H I column density of 5.5×10^{20} atoms cm^{-2}.

The implications of these flux density limits are clearest for the optically detected feature A (Keel 1988), for which a radio to X-ray spectrum (Table 2 and Fig. 2) can be constructed using the present results, the radio data of Perley et al. (1984a) and Birkinshaw et al. (1993), and the optical data of Keel. It is clear from Figure 2 that the radio spectrum of feature A in NGC 6251 is closely similar to that of knot A in M87 (with radio spectral indices $\alpha_R \approx 0.5$), but that the optical spectra differ greatly, with M87 knot A having a much flatter (bluer) spectrum (with $B-V \approx 0.6$ mag) than feature A in NGC 6251 (which has $B-V \approx 1.3$ mag, similar to the color of a late-type galaxy). The X-ray to radio flux density ratio for knot A in M87, $S_{1\,\mathrm{keV}}/S_{1.4\,\mathrm{GHz}} \sim 10^{-7}$ is also distinctly larger than the

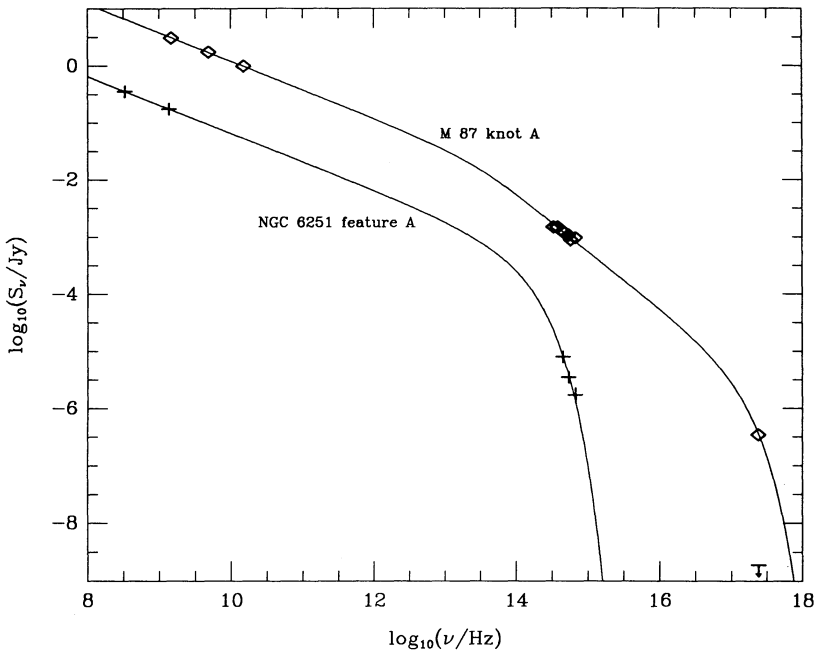

FIG. 2.—Radio to X-ray spectra of feature A in NGC 6251 (*plus signs and upper limit* [*arrow*]) and knot A in M87 (*diamonds*) constructed using the data in Table 2. For most of these points the errors are smaller than the sizes of the symbols. Note the close similarity of the slopes of the radio spectra and the relatively steeper optical spectrum of NGC 6251. The solid lines represent rough fits to these spectra from the synchroton emission of model electron energy distribution functions. The fit for NGC 6251 feature A is based on a simple power-law electron energy distribution that is cut off at energies $E > E_{\max}$, while the model distribution for M87 knot A also possesses a break of unity in the electron energy index (and hence a break of 0.5 in the photon spectrum) at intermediate energy $0.02E_{\max}$, which may be related to electron aging, although the location and size of the break are poorly constrained.

limit $S_{1\,\mathrm{keV}}/S_{1.4\,\mathrm{GHz}} < 1.1 \times 10^{-8}$ for feature A in NGC 6251. If the NGC 6251 jet had the same X-ray luminosity as the M87 jet, feature A would have been detected with a 1 keV flux density ~ 6 nJy, and if the radio to X-ray spectral ratio had been the same, it would have been a relatively bright feature, at about 20 nJy.

While the effects of differential reddening might cause an optical spectrum like that in M87 knot A to resemble the spectrum of NGC 6251 feature A, the necessary extinction, $A_V \sim 3$ mag, is much greater than expected at Galactic latitude 31°, would cause the elliptical galaxy to appear redder than it is, and would also correspond to a large line-of-sight hydrogen column (if the dust/gas ratio is normal, a column with $N_{\mathrm{H}} \approx 6 \times 10^{21}$ cm^{-2} would be expected). If the apparent spectrum of NGC 6251 feature A is dereddened by this A_V, and the effect of the associated equivalent neutral hydrogen column is removed from the X-ray flux, then its overall intrinsic spectrum might match that of M87 knot A. However, the known patchy obscuration and dust features of NGC 6251 (Nieto et al. 1983) are not close to the jet, and neither the Galactic H I survey of

TABLE 2

SPECTRA OF NGC 6251 FEATURE A AND M87 KNOT A[a]

BAND	FREQUENCY (Hz)	FLUX DENSITY (Jy)		REFERENCES
		NGC 6251 Feature A	M87 Knot A	
Radio, P	3.3×10^8	$(3.6 \pm 0.2) \times 10^{-1}$	...	BZHR
Radio, L	1.4×10^9	$(1.8 \pm 0.1) \times 10^{-1}$	(3.1 ± 0.1)	PBW, BSH
Radio, C	4.9×10^9	...	(1.7 ± 0.1)	BSH
Radio, U	1.5×10^{10}	...	(1.0 ± 0.1)	BSH
Optical, *I*	3.3×10^{14}	...	$(1.5 \pm 0.1) \times 10^{-3}$	K
Optical, *i*	3.8×10^{14}	...	$(1.5 \pm 0.1) \times 10^{-3}$	BSH
Optical, *R*	4.5×10^{14}	$(8.0 \pm 0.5) \times 10^{-6}$	$(1.3 \pm 0.1) \times 10^{-3}$	K
Optical, *r*	4.5×10^{14}	...	$(1.2 \pm 0.1) \times 10^{-3}$	BSH
Optical, *V*	5.4×10^{14}	$(3.5 \pm 0.5) \times 10^{-6}$	$(1.1 \pm 0.1) \times 10^{-3}$	K
Optical, *g*	5.8×10^{14}	...	$(9.0 \pm 2.0) \times 10^{-4}$	BSH
Optical, *B*	6.7×10^{14}	$(1.7 \pm 0.5) \times 10^{-6}$	$(1.0 \pm 0.1) \times 10^{-3}$	K
X-ray, 1 keV	2.4×10^{17}	$< 1.9 \times 10^{-9}$	$(3.4 \pm 0.2) \times 10^{-7}$	Present, BSH

NOTE.—NGC 6251 lies at a distance of about 150 Mpc, while M87 is taken to be at a distance of 20 Mpc. Feature A in NGC 6251 is thus about 3 times more luminous in the radio, and 6 times less luminous in the optical, than is knot A in M87.

[a] The spectra for these two features are plotted together in Fig. 2.

REFERENCES FOR FLUX DENSITIES.—BZHR: Birkinshaw et al. 1993; PBW: Perley et al. 1984a; BSH: Biretta et al. 1991; K: Keel 1988; Present: present work.

Stark et al. (1992) nor the survey of H I in NGC 6251 by van Gorkom et al. (1989) is consistent with the necessary reddening and X-ray absorption. Thus the observed spectral differences reflect intrinsic differences in the spectra of these jets.

The striking difference between the spectra can then be attributed to differences in the magnetic field or in the distribution function of relativistic electrons in the two regions, since these factors control the appearance of the (assumed) synchrotron emission from the jets. Figure 2 indicates that an acceptable fit to the overall shape of the spectrum of NGC 6251 feature A can be produced by a single truncated power-law distribution of electron energies which produces a cutoff frequency of about 10^{14} Hz (in rough agreement with the cutoff frequency fitted by Keel 1988), corresponding to electrons with energy $\approx 10^{12}$ eV in the ~ 20 μG equipartition field (Perley et al. 1984a) of the jet. While the photon spectrum of M87 knot A extends to much higher frequencies than that of NGC 6251 feature A, this is caused more by the larger magnetic field in this region (the equipartition field is about 400 μG; Owen et al. 1989) than by higher electron energies; the electron energy distribution in M87 knot A need extend only to $\sim 2 \times 10^{12}$ eV. It is interesting to note that the maximum electron energies are very similar (and $\approx m_p^2 c^2/m_e$) in these two regions, suggesting that electron acceleration is terminated by the same process in both jets. The synchrotron loss time of the highest energy electrons in NGC 6251 feature A is about 5×10^4 yr, comparable to the light travel time to feature A from the nucleus of the galaxy, so that electron acceleration is not required in this part of the jet: if the flow is relativistic, sufficient high-energy electrons can be advected from the nucleus to feature A. This is not the case in the jet of M87, where the synchrotron loss times for the highest energy electrons are much shorter than the light travel time, and the obvious break in the radiation spectrum (Fig. 2) may be related to the synchrotron aging of the highest energy electrons in this jet.

4. THE RADIAL STRUCTURE OF THE SOURCE

Figure 1 indicates that the X-ray source is not obviously extended on a scale larger than the full width at half-maximum (FWHM $\approx 25''$) of the *ROSAT* PSPC point response function (PRF), and a cursory examination of the image suggests that it is approximately circularly symmetric. In the present section these impressions will be quantified, and interpreted in terms of the angular size of the X-ray source associated with the core of the galaxy and the intensity of X-ray emission from an extended atmosphere of NGC 6251. This in turn will provide information on the structure of the atmosphere near the radio jet.

4.1. *The Angular Extent of the Source*

The circular symmetry of the X-ray source associated with NGC 6251 has been tested by constructing the radial profiles of the X-ray counts in four independent quadrants about the source centroid determined by the SASS (§ 2). Since these four radial profiles are consistent to the level expected from the counting statistics, we can conclude both that the SASS centroid is accurate and that the source shows no azimuthal asymmetry. In the analysis that follows, the SASS centroid is adopted, and we assume that the apparent circular symmetry of the source arises from the spherical symmetry of the underlying emission region and the circularly symmetric PRF.

A detailed comparison of the radial profile of the NGC 6251 X-ray source about its centroid with the PRF produced by the *ROSAT* telescope and PSPC is complicated by the strong energy dependence of the PRF. Thus a knowledge of the intrinsic spectrum of the source, as well as excellent in-flight calibration data, are required to make the most precise test of whether the source is extended. However, in the present case this problem is considerably simplified by the narrow distribution of counts in energy bins (see § 5) near 1 keV, which is close to the energy at which the PRF of the system is a minimum. Thus a first indication of the angular extent of the source can be obtained by a comparison of the width of the radial profile extracted from Figure 1 with the preflight, on-axis FWHM, which is approximated by

$$\mathrm{FWHM} = [409.65(E/\mathrm{keV})^{-1} + 69.27(E/\mathrm{keV})^{2.88} + 66.29]^{1/2} \text{ arcsec} . \quad (1)$$

The minimum FWHM ($23''$) occurs at $E = 1.2$ keV, and the FWHM lies in the range $23''$–$26''$ for the energy range $E = 1.0 \pm 0.3$ keV, which contains 60% of the total counts from the source. When the distribution of counts within $1'$ of the centroid of the X-ray source (relative to a background taken from an annulus between $2'$ and $3'$ from the centroid) is fitted by a simple Gaussian profile, the best-fitting FWHM of the Gaussian is $27''$ (for which $\chi^2 = 35$ with 14 degrees of freedom [dof]). The corresponding intrinsic angular size of the source is about $15''$, but the poorness of the fit and the significant energy dependence of the PRF renders this useful only as a rough upper limit to the angular size of the source in NGC 6251.

A more detailed modeling of the structure and energy dependence of the PRF is possible using Hasinger et al.'s (1992) analytical expressions for the on-axis scattering, focus, and intrinsic detector resolution contributions to the PRF as a function of energy. Although the model is based on prelaunch data, it has been found to provide reasonable fits to the early in-flight data for energies between 0.15 and 1.95 keV. The analytical expressions have been applied to the data for NGC 6251 from spectral channels 6–29 (energies 0.2–1.9 keV), which include 97% of the counts from the source, to compute a model PRF with an energy weighting that reflects the apparent energies of the detected photons. Figure 3*a* shows a comparison of the model point-spread function with the data, as found with background estimated from the annulus between $3'$ and $5'5$ from the center of the souce. The model and data profiles are consistent at the 27% level ($\chi^2 = 50.4$ with 45 dof), indicating that the source may be regarded as unresolved at this significance level. However, the pattern of residuals in the fit (Fig. 3*b*) shows evidence for some extension of the source (or an imperfection in our knowledge of the PRF of the PSPC) in the systematic depression of the residuals within $15''$ from the center and in the excess signal outside $30''$.

A model-independent angular size for the source may be obtained by fitting the radial profile with the model PRF broadened by a factor s (in the intrinsic instrument response and focus terms; the scattering term cannot be dealt with in this fashion). A good fit to the radial profile was found with a broadening factor $s = 1.027$, and the 99% confidence range for s includes $s = 1.0$ and extends to $s = 1.075$. The corresponding best-fit FWHM of the source is $\theta_h \sim 6''$, about one-quarter of the total FWHM, and the 99% upper confidence limit to the angular size is $\theta_h \lesssim 10''$. Because of the preliminary nature of the PRF model, and the likelihood that the PRF may be broadened by residual errors in the de-wobbling, we adopt the

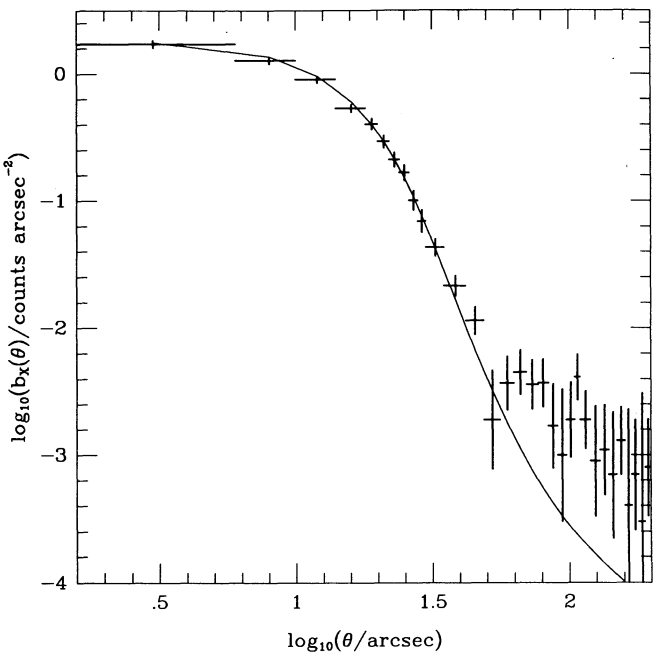

FIG. 3a

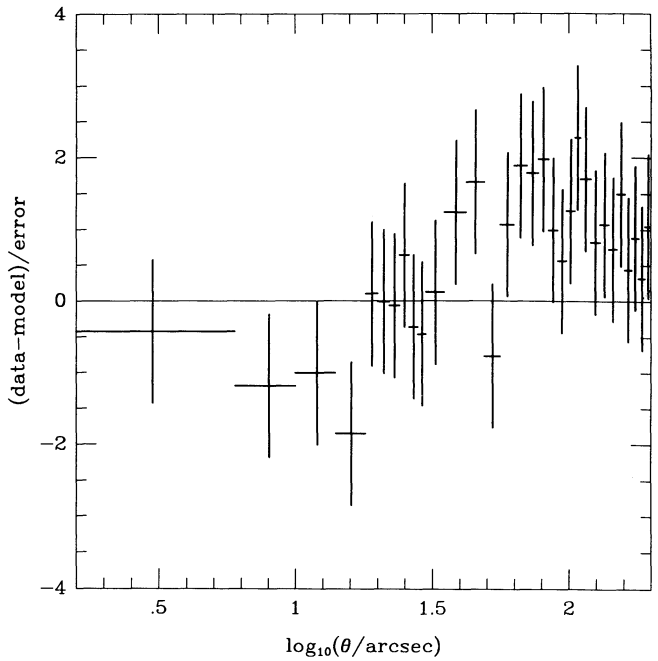

FIG. 3b

FIG. 3.—(*a*) Radial profile of surface density of counts, b_X, as a function of angle, θ, for the central source in NGC 6251 within 200″ of its center, after background subtraction, compared with the PRF of the *ROSAT* PSPC normalized to the same number of total counts. The agreement is acceptable at the 27% level. (*b*) Residuals from the comparison of the PRF of the *ROSAT* PSPC and the surface density of counts. Although the quality of the fit is acceptable, the residuals show systematic deviations above the point-source model at angles $\theta > 30''$ and below the model at angles $\theta < 15''$, suggesting the presence of some extension in the source.

upper limit

$$\theta_h < 10'' \tag{2}$$

as a model-independent angular size of the central source.

It will also be of interest to consider a model-dependent estimate of the angular size of the source. Suppose that the X-rays from NGC 6251 are thermal bremsstrahlung from a spherically symmetric distribution of hot gas with proton number density of the form

$$n_p = n_{p0}\left(1 + \frac{r^2}{r_{cx}^2}\right)^{-3\beta/2} \tag{3}$$

and constant electron temperature T_e (the conventional isothermal β model of an atmosphere; Cavaliere & Fusco-Femiano 1978). Then the X-ray surface brightness of the source is

$$b_X = \frac{\Lambda(E, T_e)}{4\pi\, d\Omega\, D_L^2} \int n_e n_p\, dV\ , \tag{4}$$

where the integral is over a cylindrical volume element along the line of sight, $dV = D_A^2\, dz\, d\Omega$, which subtends solid angle $d\Omega$ at the observer, $\Lambda(E, T_e)$ is the emissivity at photon energy E of gas at temperature T_e, and D_A and D_L are the angular diameter and luminosity distances of NGC 6251. If $n_e \propto n_p$, this integral can be performed to show that the observed angular form of the X-ray surface brightness will be

$$b_X = b_0\left(1 + \frac{\theta^2}{\theta_{cx}^2}\right)^{1/2 - 3\beta}\ , \tag{5}$$

where $\theta_{cx} = r_{cx}/D_A$ is the angular core radius of the source and b_0 is its central X-ray surface brightness.

Although equation (5) was derived on the assumption that the X-ray emission originated in a hot gas, it provides a useful model that can be fitted to the radial profile of the source in NGC 6251 whatever the origins of that source. In fitting the radial profile with a function of this form, the data are compared with the convolution of equation (5) with the (energy-dependent) *ROSAT* PRF, and then corrected for the emission from this model that lies in the 3′–5′.5 annulus about the center of the source which was used as the background region in deriving the radial distribution of counts. The *ROSAT* PRF is taken from Hasinger et al. (1992) again, and the energy dependence is represented by the distribution of counts in the spectrum of the central source.

For an assumed $\beta = \frac{2}{3}$, a best fit is found with $\theta_{cx} = 1''.0 \pm 0''.5$, although the quality of the fit is only marginally superior to the fit to a point source ($\chi^2 = 41.2$ with 43 dof, corresponding to a 55% probability of obtaining a larger value of χ^2 by chance). This fit (illustrated in Fig. 4) is qualitatively unchanged from the point-source fit of Figure 3 outside 30″ from the center of the source, but has improved in the inner parts of the radial profile. Once again the residual uncertainties in the pointing of the telescope and the PRF lead us to interpret this best fit in terms of a 3 σ upper limit

$$\theta_{cx} < 2''.5 \tag{6}$$

to the angular core radius. Attempts to fit the source with other values of β are also possible, and lead to slightly different results, but the angular FWHM of the X-ray structure,

$$\theta_h = 2\theta_{cx}(2^{2/(6\beta - 1)} - 1)^{1/2} < 4''\ , \tag{7}$$

changes little as β is varied because the radial profile can be used to constrain only a single structural parameter of a model that is much smaller than the PRF of the PSPC.

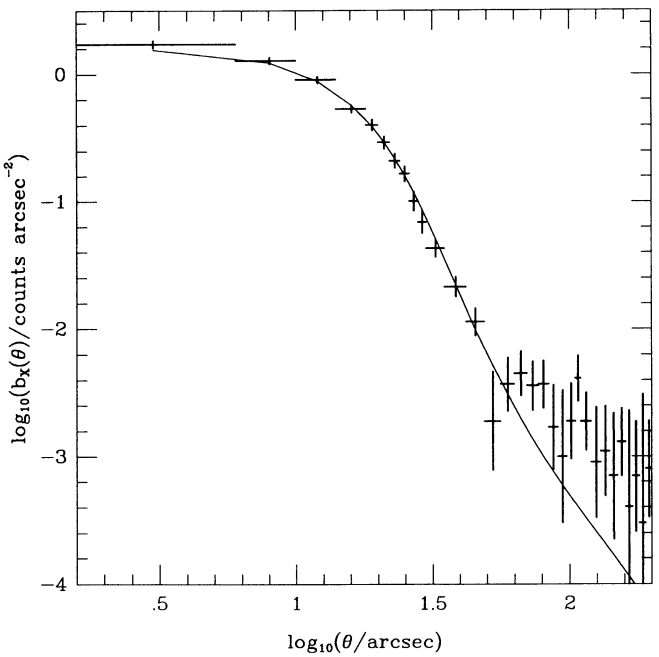

FIG. 4a

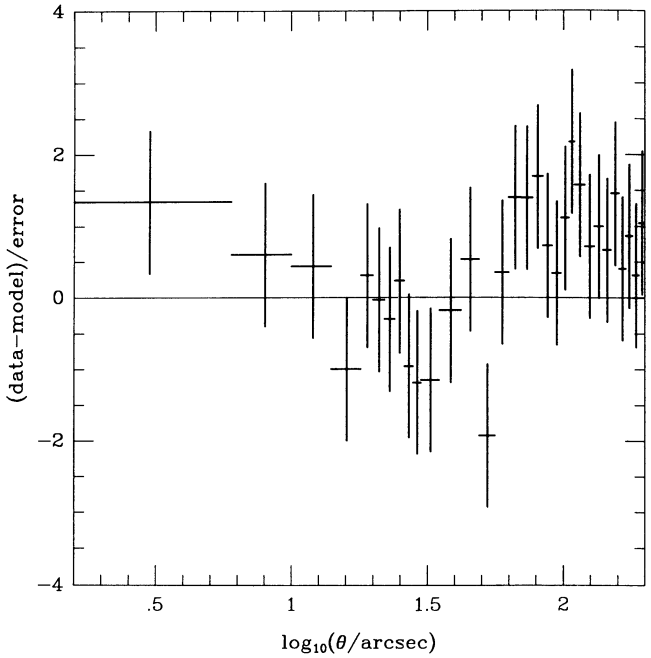

FIG. 4b

FIG. 4.—(*a*) Radial profile of surface density of counts, b_X, as a function of angle, θ, for the central source in NGC 6251 within 200″ of its center, after background subtraction, compared with the convolution of the PRF of the *ROSAT* PSPC with an isothermal β-model distribution of counts (eq. [5]) with $\beta = \frac{2}{3}$ and $\theta_{cx} = 1''$. The agreement between the model and the data is acceptable at the 55% level. (*b*) Residuals from the comparison of the surface density of counts with the model in (*a*). Although the quality of the fit is improved over the point-source fit in Fig. 3, there remain systematic deviations above the point-source model at angles $\theta > 30''$.

At the distance of NGC 6251, $1' \approx 41$ kpc, so that the X-ray source occupies a small fraction of the volume of the optical galaxy, whether the model-independent upper limit (eq. [2]) or the model-dependent limit (eq. [7]) is used. If the X-ray source is attributed to emission from a hot atmosphere, then that atmosphere is smaller in linear scale than the atmospheres in the galaxies discussed by Forman et al. (1985), and we cannot rule out the possibility that the source is confined entirely to the nucleus of the galaxy. Thus some, or all, of the emission from NGC 6251 may be interpreted in terms of a point source at the center of the galaxy.

4.2. *Limits to the Pressure in the Environment of the Kiloparsec-Scale Radio Jet*

Figures 3 and 4 suggest that the radial profile of X-ray emission from NGC 6251 contains a significant number of counts from a component with angular size $\gtrsim 20''$. If we interpret this as the thermal bremsstrahlung from a galactic atmosphere, then it is this component of the X-radiation that traces the medium whose pressure may confine the kiloparsec-scale radio jet. In this section we model the radial profile as the superposition of a nuclear point source and an extended halo in order to estimate the density and pressure of this component of the X-ray source.

Once again, we suppose that the proton density in an atmosphere of NGC 6251 is described by an isothermal β-model with a density law of the form of equation (3). Information on the properties of this gas is obtained through analysis of the X-ray surface brightness of the emission, given by equation (5). If the emissivity of the gas takes account of the energy response of the detector, and the necessary cosmological corrections for energy and time, the surface brightness can be converted to the more convenient quantity

$$\mathscr{A} = \frac{\int n_e n_p dV}{4\pi\, d\Omega\, D_L^2}\,, \tag{8}$$

which is the distance-normalized volume emission measure of the atmosphere per unit solid angle. $\mathscr{A}$ is obtained from the observed surface brightness count rate by taking account of the absorption of the X-radiation in our Galaxy, the temperature of the atmosphere, and the energy-dependent response of the PSPC. The angular structure of the distance-normalized volume emission measure is of the same form as equation (5),

$$\mathscr{A}(\theta) = \mathscr{A}_0\left(1 + \frac{\theta^2}{\theta_{cx}^2}\right)^{1/2 - 3\beta}\,, \tag{9}$$

where the central normalization is given by

$$\mathscr{A}_0 = \pi^{1/2}\,\frac{\Gamma(3\beta - 1/2)}{\Gamma(3\beta)}\,\eta n_{p0}^2\,\frac{D_A^2}{4\pi D_L^2}\,r_{cx}\,, \tag{10}$$

and $\eta = n_e/n_p$ is the electron-to-proton ratio in the atmosphere (assumed constant). If the gas has normal cosmic composition, $\eta = 1.18$.

The value of the central surface brightness of the gaseous halo, b_0, or the central distance-normalized volume emission measure, $\mathscr{A}_0$, can be obtained by fitting a model composed of equation (9) plus an unresolved point source at the nucleus, convolved with the energy-dependent PSPC PRF (obtained as in § 4.1) to the radial distribution of counts. The simpler fits of Figures 3 and 4 suggest that this procedure will detect a significant halo at a surface brightness of about 0.2% of the central surface brightness of the source. At this level, some of the signal could arise from uncertainties in the PRF of the PSPC,

although no such systematic errors are apparent in the in-flight check of the PRF performed by Hasinger et al. (1992) in the 0.2–1.9 keV energy band that we use for our fits.

The results from a variety of β-models (with $\beta = \frac{1}{2}, \frac{2}{3}$, and $\frac{3}{4}$ and core radii 1, 2, 5, 10, 20, and 50 kpc, spanning the range of structures seen in nearby elliptical galaxies; Forman et al. 1985) are given in Table 3, which lists, for each of the 18 models fitted, the fraction of the source counts in the point-source component (f_p) and the central surface brightness of the β-model component expressed both in terms of the PSPC counts (b_0) and in terms of the distance-weighted volume emission measure $\mathscr{A}_0$. Good fits are obtained for cases where a β-model component of large angular size provides a small fraction of the counts in the source, since these models describe the brightness excess at large angles from the source center without affecting the quality of the fits at small radius (e.g., Fig. 5). There is a large improvement in the value of χ^2 from the results of Figures 3 and 4 (or the models in Table 3 with small values of r_{cx}) when an extended β-model is added; the fit in Figure 5 (with $\beta = \frac{2}{3}$ and $r_{cx} = 50$ kpc) has $\chi^2 = 27.6$ with 41 dof. However, the peak surface brightness of this extended component is only 0.3% of the peak surface brightness in the source, so that the estimate of b_0 for this component is strongly dependent on the accuracy of the PRF of the PSPC. Thus, while the evidence for an extended X-ray component in NGC 6251 is strong, the measured values of b_0 in Table 3 may overestimate its brightness slightly. The best-fitting β-models (which have χ^2 values slightly less than those of the largest models in Table 3) have core radii $r_{cx} = 75$–100 kpc, corresponding to an FWHM $\approx 3'$ for the extended component of the source.

Formally, isothermal β-models with values of $\beta \leq \frac{2}{3}$ are not acceptable, since they correspond to infinite masses of gas in the galaxies, and the model gas distribution (eq. [3]) should be truncated at some outer radius. However, the effect of such a truncation on the model emission measure distribution (eq. [9]) will be small, provided that the truncation is made at several r_{cx}, and equation (9) will be sufficiently accurate for our present purposes.

For any choice of β and r_{cx} in Table 3, the value of $\mathscr{A}_0$ can be used to estimate the central gas density associated with the extended atmosphere (which should be distinguished from the central gas density that might be associated with the unresolved core source), and hence the pressure at any point within the atmosphere. If the kiloparsec-scale jet in NGC 6251 is oriented at angle i to the line of sight (at $i = 0°$ the jet lies along the line of sight, and at $i = 90°$ it lies in the plane of the sky), the external pressure on the jet at an observed angle θ from the core of the galaxy is

$$P_{\rm ext}(\theta) = \frac{k_{\rm B} T_e}{\mu m_{\rm H}} \rho(r_\theta) , \tag{11}$$

where μ is the mass per particle in the gas (in units of the mass of a hydrogen atom; $\mu = 0.60$ for a gas with normal cosmic abundance), $m_{\rm H}$ is the mass of a hydrogen atom, $k_{\rm B}$ is Boltzmann's constant, T_e is the electron temperature of the gas (assumed constant over the atmosphere), and $\rho(r_\theta)$ is the density of gas at a point

$$r_\theta = \frac{D_A \theta}{\sin i} \tag{12}$$

from the center of the galaxy. The density ρ is related to the proton number density by

$$\rho(r) = \frac{m_{\rm H} n_p(r)}{X} , \tag{13}$$

where X is the abundance of hydrogen by mass (0.74 for normal cosmic abundances). Combining these results, and using equation (10) for $\mathscr{A}_0$, we deduce that the ambient pressure on the jet at an apparent angle θ from the center of

TABLE 3

X-RAY BRIGHTNESS OF POINT-SOURCE AND β-MODEL ATMOSPHERE IN NGC 6251

β	r_{cx} (kpc)	f_p[a]	b_0 (counts s^{-1} arcmin^{-2})	$\mathscr{A}_0$[b] (10^{10} cm^{-5} arcmin^{-2})
0.500.....	1	0.85 ± 0.03	0.96 ± 0.16	53 ± 9
0.500.....	2	0.87 ± 0.03	0.24 ± 0.05	13 ± 3
0.500.....	5	0.90 ± 0.03	0.041 ± 0.009	2.3 ± 0.5
0.500.....	10	0.91 ± 0.03	0.012 ± 0.003	0.64 ± 0.14
0.500.....	20	0.93 ± 0.03	0.0039 ± 0.0008	0.21 ± 0.05
0.500.....	50	0.94 ± 0.03	0.0013 ± 0.0003	0.073 ± 0.015
0.667.....	1	0.49 ± 0.03	14 ± 1	760 ± 40
0.667.....	2	0.71 ± 0.03	1.9 ± 0.2	100 ± 10
0.667.....	5	0.85 ± 0.03	0.16 ± 0.03	8.8 ± 1.7
0.667.....	10	0.89 ± 0.03	0.029 ± 0.007	1.6 ± 0.4
0.667.....	20	0.92 ± 0.03	0.0068 ± 0.0017	0.37 ± 0.09
0.667.....	50	0.94 ± 0.03	0.0017 ± 0.0004	0.094 ± 0.020
0.750.....	1	0.13 ± 0.03	35 ± 1	1900 ± 100
0.750.....	2	0.60 ± 0.03	3.9 ± 0.3	220 ± 20
0.750.....	5	0.82 ± 0.03	0.26 ± 0.04	14 ± 2
0.750.....	10	0.88 ± 0.03	0.041 ± 0.010	2.3 ± 0.6
0.750.....	20	0.91 ± 0.03	0.0085 ± 0.0022	0.47 ± 0.12
0.750.....	50	0.93 ± 0.03	0.0019 ± 0.0004	0.11 ± 0.02

[a] The quantity f_p is the fraction of the total X-ray flux from NGC 6251 (of 0.10 PSPC counts s^{-1}) that is contained in the point-source component.

[b] The conversion from b_0 to $\mathscr{A}_0$ is made under the assumption that the temperature of the atmosphere is $k_B T_e = 1$ keV and that the neutral hydrogen column is $N_{\rm H} = 5.5 \times 10^{20}$ cm^{-2}, the value from the Galactic H I survey of Stark et al. 1992.

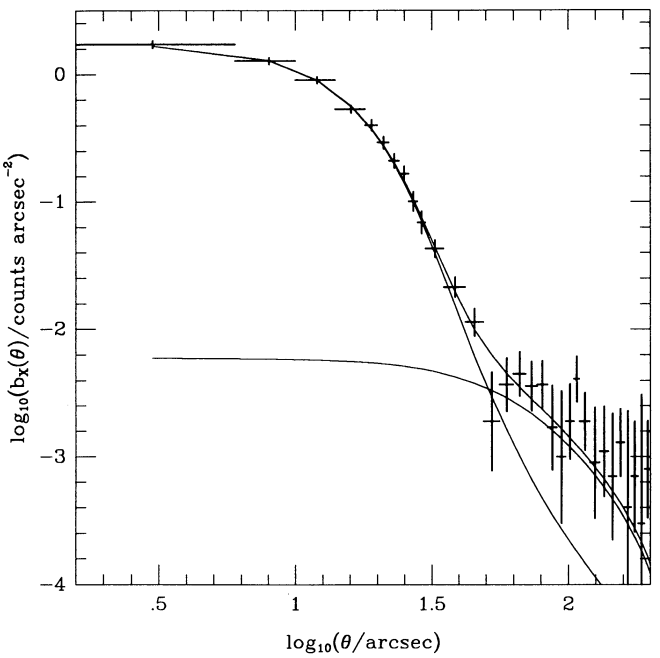

FIG. 5a

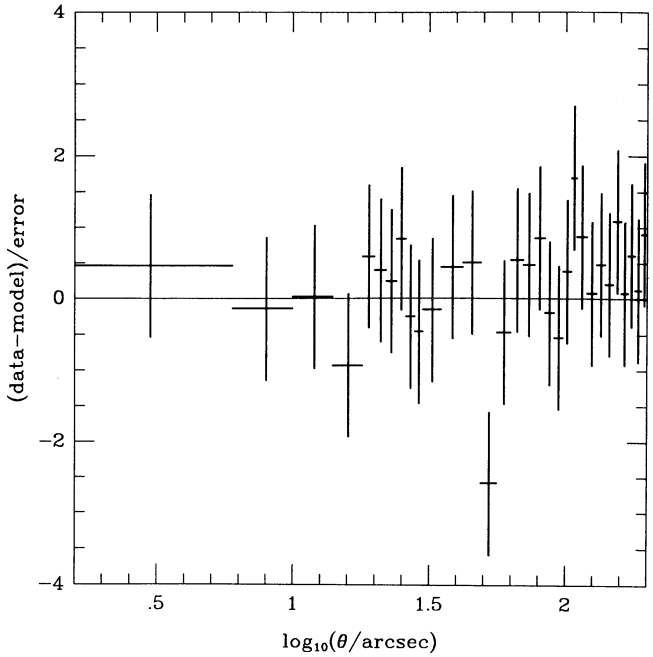

FIG. 5b

FIG. 5.—(*a*) Radial profile of surface density of counts, b_X, as a function of angle, θ, for the central source in NGC 6251 within 200″ of its center position, after background subtraction, compared with the convolution of the PRF of the *ROSAT* PSPC with the superposition of a point source and an isothermal β-model distribution of counts (eq. [5]) with $\beta = \frac{2}{3}$ and $\theta_{cx} = 72''$ ($r_{cx} = 50$ kpc). The upper curve shows the total model, while the bright, small angular size and fainter, large angular size curves represent the contributions from the point-source and β-model components, respectively. The probability of obtaining worse agreement between data and model by chance is 95%. (*b*) Residuals from the comparison of the surface density of counts with the model in (*a*). There remain no large angular scale systematic deviations between the model and the data.

NGC 6251 is

$$P_{\rm ext}(\theta) = \frac{k_{\rm B} T_e}{\mu X}\left[\frac{\mathscr{A}_0}{\eta}\frac{D_L^2}{D_A^3\theta_{cx}}\frac{4\pi^{1/2}\Gamma(3\beta)}{\Gamma(3\beta - 1/2)}\right]^{1/2} \times\left(1 + \frac{\theta^2}{\theta_{cx}^2 \sin^2 i}\right)^{-3\beta/2}. \quad (14)$$

The greatest possible external pressure on the jet, and hence the strongest possibility of external pressure confinement, occurs for $i = 90°$, when the jet is in the plane of the sky and observed angular separations of jet features from the core of the galaxy correspond to minimum linear distances. Table 4, which gives the external pressures at each of features A–D in the jet, is therefore calculated for $i = 90°$. The temperature of the atmosphere was taken to be 1 keV, representative of the temperatures found by Forman et al. (1985) and Kim, Fabbiano, & Trinchieri (1992), and somewhat higher than the temperature of the possible cool component in the spectrum of the core (§ 5). If a higher temperature is assumed, then the external pressure would be higher: the pressures given in Table 4 can be scaled to higher temperatures using

$$\frac{P_{\rm ext}(T_e)}{P_{\rm ext}(1\ {\rm keV})} = \begin{cases} 3.2\,, & k_{\rm B} T_e = 2\ {\rm keV}\,, \\ 5.5\,, & k_{\rm B} T_e = 3\ {\rm keV}\,, \\ 7.4\,, & k_{\rm B} T_e = 4\ {\rm keV}\,, \\ 9.5\,, & k_{\rm B} T_e = 5\ {\rm keV}\,, \end{cases} \quad (15)$$

which takes account of the temperature dependence of Λ (present in $\mathscr{A}_0$) as well as the factor T_e in equation (14).

The pressures in Table 4 are to be compared with the internal pressure of the NGC 6251 jet. Perley et al. (1984a) give minimum internal energy densities $u_{\rm min}$ at various points down the jet. The corresponding minimum internal pressures of relativistic material inside the jet, $P_{\rm min} = \frac{1}{3}u_{\rm min}$, corrected to the distance scale that we have adopted, are given in the column headings of Table 4. It can be seen that none of features A–D in the jet can be confined by external pressure if the temperature of the halo is 1 keV: the X-ray surface brightness of a confining atmosphere at this temperature would have been relatively bright on Figure 1. If the temperature of the atmosphere is as high as 3 keV, then feature A in the jet (which lies between 10″ and 40″ from the nucleus) can be confined by the external gas if the jet is in the plane of the sky: the remainder of the jet is then free. If the halo gas has a temperature of 5 keV, then most of the jet can be pressure-confined for some of these models if the jet lies close to the plane of the sky (e.g., for the $\beta = \frac{2}{3}$, $r_{cx} = 10$ kpc model, feature A is confined if $i \gtrsim 30°$, features B and C are confined if $i \gtrsim 70°$, and feature D cannot be confined by the pressure of the atmosphere). It is interesting to note that our results indicate that feature A is most easily confined, whereas the other features can be confined only if the halo is hot and the jet lies close to the plane of the sky. This conclusion is opposite to that reached by Perley et al. (1984a), based on the morphological properties of the jet, that feature A is free while the jet is confined at features B, C, D, and beyond. Note that this conclusion is almost independent of the cosmological distance scale: for a jet with radio spectral index α (defined in the sense $S_\nu \propto \nu^{-\alpha}$) the minimum-energy estimate is proportional to $D_A^{-2/(3+\alpha)}$, so that for the jet of NGC 6251 ($\alpha = 0.64 \pm 0.05$; Perley et al. 1984a) the minimum internal pressure $P_{\rm min} \propto D_A^{-0.55}$, very close to the $P_{\rm ext} \propto D_A^{-0.50}$ distance dependence of equation (14).

Can the external medium be hot enough to confine the jet? If any of the jet features is to be confined, the temperature of the

TABLE 4

EXTERNAL PRESSURE ON THE RADIO JET OF NGC 6251

β	r_{cx} (kpc)	n_{p0} (10^{-3} cm^{-3})	$P_{ext}/10^{-12}$ N m^{-2} [a] Feature A (min = 1.5)[b]	Feature B (min = 0.6)[b]	Feature C (min = 0.2)[b]	Feature D (min = 0.2)[b]
0.500.....	1	110 ± 10	0.55	0.10	0.038	0.019
0.500.....	2	39 ± 4	0.55	0.10	0.038	0.019
0.500.....	5	10 ± 1	0.54	0.10	0.039	0.019
0.500.....	10	3.8 ± 0.4	0.49	0.10	0.041	0.021
0.500.....	20	1.6 ± 0.2	0.37	0.11	0.047	0.023
0.500.....	50	0.58 ± 0.06	0.19	0.12	0.060	0.032
0.667.....	1	470 ± 10	0.57	0.056	0.016	0.006
0.667.....	2	120 ± 10	0.59	0.058	0.017	0.007
0.667.....	5	23 ± 2	0.63	0.066	0.019	0.007
0.667.....	10	6.8 ± 0.8	0.62	0.078	0.023	0.009
0.667.....	20	2.3 ± 0.3	0.48	0.098	0.030	0.012
0.667.....	50	0.74 ± 0.08	0.24	0.12	0.051	0.022
0.750.....	1	790 ± 10	0.47	0.034	0.008	0.003
0.750.....	2	190 ± 10	0.52	0.038	0.009	0.003
0.750.....	5	30 ± 3	0.62	0.049	0.012	0.004
0.750.....	10	8.5 ± 1.0	0.65	0.063	0.016	0.006
0.750.....	20	2.7 ± 0.4	0.53	0.087	0.023	0.008
0.750.....	50	0.82 ± 0.09	0.26	0.12	0.045	0.018

[a] The external pressures are estimated from the limits to the X-ray surface brightness of any extended halo around NGC 6251 under the assumptions that the jet is in the plane of the sky (other jet angles lead to smaller external pressures) and that the temperature of the halo gas is 1 keV. The fractional errors on these pressures are the same as the fractional error on the central proton density in the atmosphere, n_{p0}.

[b] The minimum internal pressures in these features in the jet are taken from the minimum-energy analysis of Perley et al. 1984a, adjusted to a Hubble constant of 50 km s^{-1} Mpc^{-1}. Values are $P_{min}/10^{-12}$ N m^{-2}.

gas must be at least 2 keV. If the entire jet is to be confined, then the temperature must exceed 5 keV. Now, the quantity β is supposed to be related to the properties of the gas and the confining mass by

$$\beta = \frac{\mu m_H \sigma_z^2}{k_B T_e}, \quad (16)$$

where σ_z is the line-of-sight velocity dispersion characteristic of the mass (Cavaliere & Fusco-Femiano 1978). The stellar velocity dispersion of NGC 6251 has been measured to be $\sigma_z = 293 \pm 20$ km s^{-1} (Heckman, Carty, & Bothun 1985), so that the temperature of the gas should be

$$k_B T_e = (0.54 \pm 0.07)\beta^{-1} \text{ keV}, \quad (17)$$

but the relationship between temperature and the structural β-parameter is found to be looser than indicated by the error in equation (17); in clusters of galaxies equation (16) is found to overestimate the temperature of the gas by up to a factor of 2 (this is the so-called β-discrepancy; e.g., Sarazin 1984). However, even allowing for a factor of 2 error in equation (17) *in the opposite sense*, and the full likely range of β (0.5–1.0), it is clear that NGC 6251 cannot hold an atmosphere with $k_B T_e \gtrsim 2$ keV, and hence that the maximum galactic atmosphere of NGC 6251 cannot confine the jet.

Furthermore, NGC 6251 is not associated with a cluster of galaxies capable of containing an intracluster medium as hot as 5 keV. There are a number of bright ($m_B < 15.5$ mag) galaxies close to NGC 6251, but most of these are associated with Abell 2247, a cluster that lies at a substantially larger distance than NGC 6251 (it has $cz \approx 11{,}000$ km s^{-1}; cf. 7400 km s^{-1} for NGC 6251). Within 2000 km s^{-1} of the velocity of NGC 6251 the CfA redshift survey (J. Huchra 1991, private communication) finds only nine galaxies. Five of these are associated with the Zwicky cluster Zw 1609+8212, which lies 5 Mpc in projected distance from NGC 6251 and 1000 km s^{-1} closer in redshift. The remaining galaxies lie within 1° (~2 Mpc in projected distance) of NGC 6251 and have velocities within 400 km s^{-1} of the velocity of NGC 6251 (no velocity is recorded for NGC 6252, which lies a few arcminutes north of NGC 6251). Thus the NGC 6251 group of galaxies has a velocity dispersion $\lesssim$400 km s^{-1}, covers a region 1–2 Mpc in diameter, and is not massive enough to contain a gas of temperature 5 keV.

We conclude that the outer jet (features B, C, and D, which Perley et al. 1984a believe to be confined) is not confined by the static pressure of any galactic atmosphere of NGC 6251, and that feature A (which Perley et al. 1984a believe to be unconfined) can only be confined if the atmosphere of the galaxy is hotter than suggested by its measured velocity dispersion. The jet of NGC 6251 is therefore either free, or confined by another mechanism, such as magnetic confinement (for which some support might be found in the edge-brightened polarization of the radio emission in the inner part of the jet; Perley et al. 1984a) or ram-pressure confinement produced by the overpressure inside the bow shock created by the motion of the jet (if it is hypersonic; e.g., Loken et al. 1992). This conclusion also applies if much of the radio emission originates in small-scale features within the jet: the minimum-energy argument then produces considerable underestimates of the pressure in the radio-emitting regions, and these regions will be free (and transient) or confined by internal shocks or fields in the jet. Similar conclusions about the failure of pressure confinement of the jets of a high-power radio source (Cygnus A) and a low-power radio source (M87) were reached by Perley, Dreher, & Cowan (1984b) and Owen et al. (1989), respectively, and pressure confinement has long been known to be ineffective in the lobes of double radio galaxies (e.g., Miller et al. 1985).

However, the data that we present here are the first for which the X-ray resolution is sufficient to provide a good separation of possible components on the angular scales of the core, jet, and galactic atmosphere.

The result for the density of the atmosphere around NGC 6251 is also interesting in interpreting the radio polarization data of Perley et al. (1984a), which showed the presence of strong structure in the Faraday rotation on angular scales $\sim 10''$ at angles $\sim 70''$ from the nucleus. In order for this Faraday rotation to arise from a smooth atmosphere of NGC 6251, Perley et al. (1984a) deduced that an electron density of order $0.003(B/\mu\mathrm{G})^{-1}$ cm^{-3} is required. The density of the atmosphere of NGC 6251 near this part of the jet is less than about 5×10^{-4} cm^{-3} for all the models used (Table 4; eq. [3]), so that the magnetic field in this medium must exceed 6 μG and display strong structure on kiloparsec scales if the Faraday rotation is to be understood in this fashion. This field is comparable in strength to the internal equipartition field in the jet, so that it could provide a substantial fraction of the necessary confining pressure on the jet.

5. THE NUCLEAR SOURCE

In § 4 it was shown that the dominant component of the X-ray source associated with NGC 6251 has an angular size less than the PSPC resolution. The model-independent estimate of the angular size,

$$\theta_h < 10'' , \quad (18)$$

corresponds to a source with diameter less than about 7 kpc, while the interpretation of the core source in terms of an isothermal β-model leads to

$$\theta_h < 4'' . \quad (19)$$

Further information on the nature of the X-ray emission can be obtained by fitting spectral models to the PSPC data. Our fits have been performed using the IRAF/PROS software, with the best available in-flight calibration data (released around 1992 March) for PSPC detector 2. We have restricted our fitting to PROS energy bins 2–34 (0.1–2.4 keV), for which the calibrations are indicated as being reliable. Counts were extracted by integrating the emission over a circle of 2′ radius, and subtracting the background derived from an annulus with inner radius 2′ and outer radius 4′. A total of 1521 ± 44 net counts were collected from NGC 6251.

Independent information on the spectrum of NGC 6251 was obtained from the data taken with the *Einstein Observatory* IPC for roughly equal durations in 1979 September and November and a total exposure time of 18,572 s. IPC counts were extracted from a circle of 3′ radius centered on NGC 6251, and the background was derived from an annulus with inner and outer radii of 5′ and 6′. The IPC gain was significantly different for the two time periods. However, an analysis of the separate data sets indicates consistent spectral parameters within the rather large uncertainties, and so models have been fitted to the two IPC observations simultaneously. The IPC data provide information at overlapping but somewhat higher energies than the *ROSAT* PSPC.

5.1. *Single-Component Fits to the Spectrum: The N_H Problem*

We find that a power-law spectrum with energy index $\alpha_X \sim 1.8$, hydrogen column density $N_H \sim 1.8 \times 10^{21}$ atoms cm^{-2}, and a 1 keV flux density of 8.4×10^{-4} keV cm^{-2} s^{-1} keV^{-1} (0.56 μJy) is a good representation of the PSPC data ($\chi^2 = 33.28$ with 30 dof). A single-temperature Raymond & Smith (1977) plasma gives a sufficiently bad fit that this model must be rejected ($\chi^2 = 70.5$ with 30 dof).

Despite the good fit to the power-law model, the absorbing hydrogen column is substantially larger than the Galactic $N_H = 5.5 \times 10^{20}$ atoms cm^{-2} at the position of NGC 6251 (Stark et al. 1992). We have chosen to assume that this discrepancy is due to an excess N_H at the redshift of NGC 6251; the relative closeness of the galaxy ($cz = 7400$ km s^{-1}) causes the fits to be essentially unaffected if instead the excess absorption is assumed to be in our Galaxy. For all subsequent fits we have fixed the Galactic N_H at 5.5×10^{20} atoms cm^{-2} and have allowed the intrinsic N_H to be a free parameter. The values of the parameters estimated from a fit to a power law with intrinsic absorption are given as the first entry in Table 5, and the best fit is shown in Figure 6. The results remain consistent with a steep power-law spectrum, with substantial excess absorbing column.

It is interesting to check the results of the PSPC fit using the *Einstein* IPC spectrum for NGC 6251. We find that the IPC data are marginally consistent with a single–power-law model for the X-ray emission ($\chi^2 = 27$ with 18 dof), with a fitted energy index $\alpha_X = 1.4$, an intrinsic (excess over Galactic) absorbing column at NGC 6251 of $N_H = 2.3 \times 10^{21}$ cm^{-2} (see entry 2 in Table 5). Contour plots for the IPC and *ROSAT* data are overlaid in Figure 7, where it is shown that the contours just touch. Although the two IPC observations agree with each other within their (large) errors, the PSPC spectrum is consistent only with one of the two IPC observations. This leads to the rather poor joint fit to all the data together and the fact that two-component model fits to the joint IPC and PSPC data do not significantly improve χ^2 (entry 3 in Table 5). We interpret the results as possible evidence for spectral variability between the three observations. Since the spectrum (in counts) peaks so strongly at about 1 keV, and falls off sharply both to lower and higher energies, and since the uncertainties from the IPC observations are relatively large, we have restricted further spectral fitting to the PSPC data alone.

The steepness of the power-law spectrum in these fits is somewhat unexpected. Perhaps the best comparison is with Cen A, whose variable nuclear X-ray source has a spectral index in the range 0.6–0.9 (Feigelson et al. 1981). The soft X-ray spectral indices of BL Lac objects are typically close to 1.0, and radio-loud quasars tend to have flatter spectra (Worrall & Wilkes 1990).

The excess absorption in the spectrum, corresponding to a neutral hydrogen column $\sim 1.3 \times 10^{21}$ atoms cm^{-2}, is also unusual, and the location of this excess column on the line of sight to the nucleus of NGC 6251 is unclear. It is not likely that the Galactic hydrogen at this position (Galactic coordinates l, $b = 111°, +31°$) could have sufficient small-scale structure to produce variations of a factor ≈ 3 in N_H on different lines of sight within the Stark et al. (1992) beam. The 21 cm optical depth of this gas, if it is all in the form of H I rather than H_2, against the 0.5 Jy radio core of NGC 6251 would be

$$\tau_0 = 51.5(N_H/10^{20}\ \mathrm{cm}^{-2})(T_S/\mathrm{K})^{-1}(\Delta v/\mathrm{km\ s}^{-1})^{-1} , \quad (20)$$

where T_S is the spin temperature of the gas and Δv is the velocity FWHM of the neutral hydrogen line. For $\Delta v \approx 150$ km s^{-1}, a value typical of detected elliptical galaxies, $T_S \approx 100$ K, and the inferred excess column density, this corresponds to a line with central optical depth $\tau_0 \approx 0.04$. However, van Gorkom et al. (1989) found no evidence for a neutral hydrogen

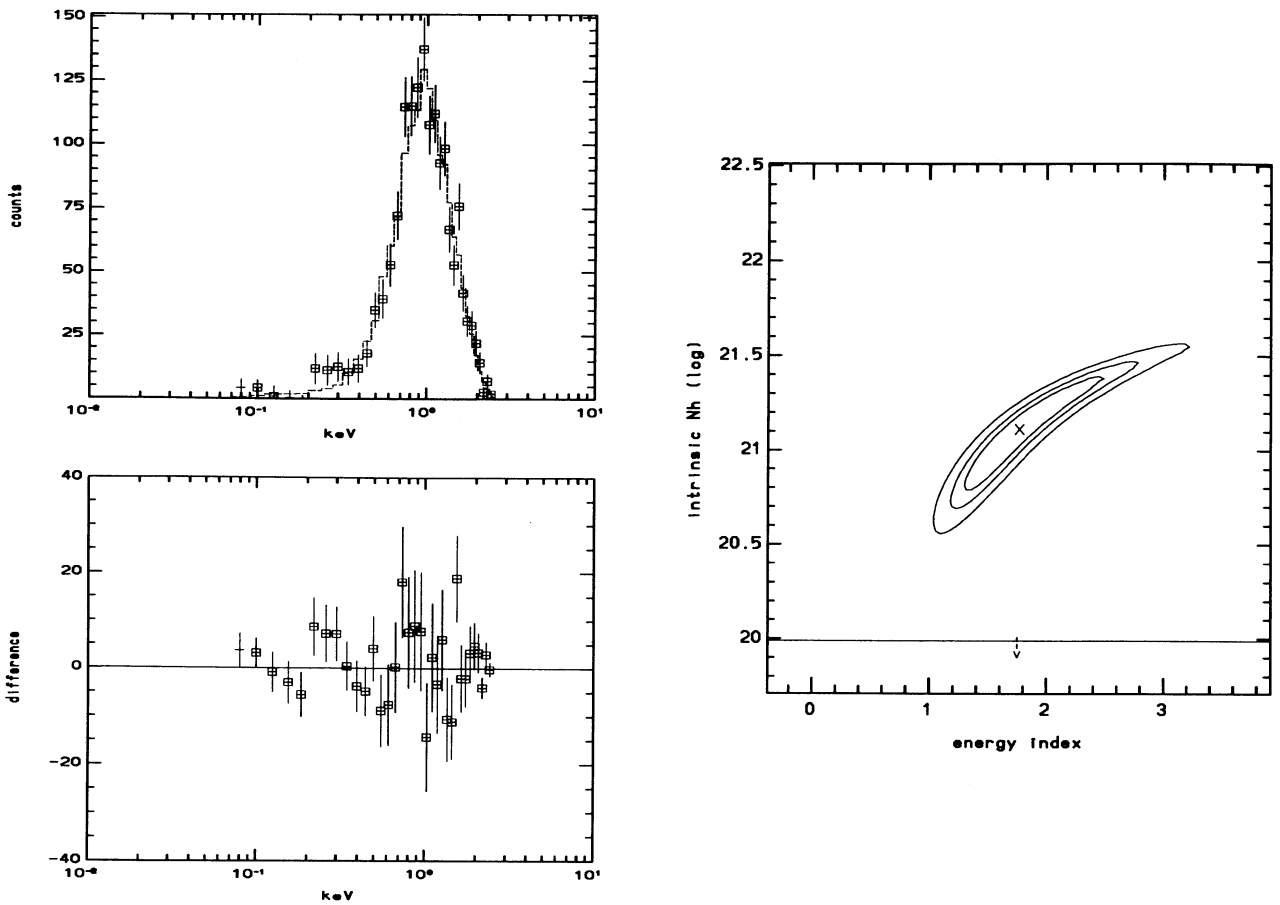

FIG. 6.—Spectral fit of the PSPC data to the model of a power law with fixed Galactic absorption and excess intrinsic absorption with $N_H = 1.3 \times 10^{21}$ cm^{-2} (entry 1 in Table 5). The panels on the left show the net counts compared with the model fit, with (data − model) in the lower plot. The figure on the right shows contours of equal χ^2 at values of 2.3, 4.6, and 9.2 above the best-fit value, corresponding to uncertainties of 1 σ, 90%, and 99%, for two interesting parameters. The projection for two of the three free parameters in the model, energy index and intrinsic absorption, is shown. Note that the known upper limit to the intrinsic N_H of 9.5×10^{19} cm^{-2} (marked by a horizontal line) is inconsistent with the X-ray data, indicating either that some as yet unmeasured absorbing gas is present or that the intrinsic spectrum of NGC 6251 is more complicated than a power law, even over the small range of energies for which the *ROSAT* spectrum shows a large number of counts.

absorption feature with $\tau_0 > 0.013$ at the redshift of NGC 6251, so that the hydrogen column, if present, occurs at a velocity outside the range (systemic velocity $\pm$ 300 km s^{-1}) which they surveyed, perhaps being due to an exceptionally massive infalling cloud or galaxy. It is not likely that the absorbing column arises from an intergalactic cloud projected across the face of NGC 6251, since the H I column is so large; the cloud in the Leo group (Schneider et al. 1983) has a column of only $N_H \approx 7 \times 10^{19}$ cm^{-2}.

It is also interesting to note that a value of N_H this high would produce significant reddening of the galaxy core. For typical dust/gas ratios and dust properties,

$$A_V \approx 0.04(N_H/10^{20}\ \text{cm}^{-2}) , \quad (21)$$

so that an intrinsic $N_H = 1.3 \times 10^{21}$ atoms cm^{-2} would produce a visual extinction of about 0.5 mag toward the center of the galaxy. CCD studies of NGC 6251 should be able to detect the flattened central brightness profile of the starlight from NGC 6251 that this would imply, but no evidence of such an effect was reported by Young et al. (1979), who found, instead, evidence for a slight blue excess in the center of the galaxy and a sharply peaked central surface brightness which they interpreted as evidence of a central black hole of mass $M_{BH} \approx 2.4 \times 10^9\ M_\odot$.

5.2. *Multicomponent Models for the Spectrum*

Since no plausible site exists for the necessary neutral hydrogen column toward NGC 6251, some other explanation should be tried to explain the form of the spectrum. One possibility is that the X-ray spectrum emitted by the core source in NGC 6251 is more complicated than a simple power law (even over the narrow energy range in which it is detected). Although a single thermal component gives an unacceptable χ^2 (see § 5.1), it exhibits the desirable feature of not requiring an excess N_H above the Galactic value. The reason for this is clear: a low-temperature ($k_B T_e \sim 0.5$ keV) gas produces a spectrum which peaks in the *ROSAT* energy band, producing a turn-down at low energies. Noting too that 0.5 keV gas is found in other elliptical galaxies (e.g., Forman et al. 1985; Kim et al. 1992) and so would not be unexpected in NGC 6251, we have fitted two-component spectral models in which one component is a thermal source.

A model consisting of a power law and Raymond & Smith (1977) thermal component gives an acceptable fit (entry 4*a* in

TABLE 5

MODEL PARAMETERS DETERMINED FROM THE SPECTRAL FITS

	Power Law $f \propto E^{-\alpha}$ μJy		Raymond-Smith Thermal 100% Cosmic Abundances		Galactic N_H	Intrinsic N_H		
Data Set/Model	α	1 keV Flux density (μJy)	$k_B T_e$ (keV)	Emission Measure/$4\pi D_L^2$ (10^9 cm^{-5})	10^{20} cm^{-2} (fixed)	10^{20} cm^{-2}	χ^2/dof	Comments
(1) PSPC/power law	$1.8^{+0.7}_{-0.5}$	$0.55^{+0.22}_{-0.11}$	...	...	5.52	13^{+12}_{-7}	33.0/30	Intrinsic N_H exceeds van Gorkom et al. 1989 upper limit of 0.95×10^{20} cm^{-2}; spectrum anomalously steep; see Figs. 6 and 7
(2) IPC/power law	$1.4^{+1.4}_{-0.9}$	$0.6^{+1.4}_{-0.4}$	...	...	5.52	23^{+40}_{-21}	27.0/18	Acceptable only at 7% significance level; see Fig. 7
(3) PSPC and IPC/power law	$1.3^{+0.4}_{-0.3}$	$0.47^{+0.09}_{-0.06}$	...	...	5.52	8^{+6}_{-3}	77.6/51	Acceptable only at 1% significance level; the following models offer no significant improvement in fit: (*a*) two power laws: 70.9/49; (*b*) power law and thermal: 69.9/49; (*c*) two thermals 71.5/49
(4*a*) PSPC/power law and thermal	$1.0^{+0.6}_{-0.5}$	$0.37^{+0.13}_{-0.07}$	$0.53^{+0.31}_{-0.25}$	$7^{+24.0}_{-4.5}$	5.52	$5.0^{+9.0}_{-3.2}$	27.6/28	Plausible model with small excess N_H.
(4*b*) PSPC/power law and thermal	$0.27^{+0.18}_{-0.27}$	$0.26^{+0.03}_{-0.04}$	$0.49^{+0.13}_{-0.11}$	10^{+6}_{-3}	5.52	...	34.6/29	Plausible model with no excess N_H; see Fig. 8
(5*a*) PSPC/two thermals	...	...	$0.37^{+0.17}_{-0.09}$ and $3.3^{+3.9}_{-1.1}$	19^{+27}_{-10} and 145^{+22}_{-17}	5.52	$2.4^{+5.2}_{-1.9}$	27.4/28	Hotter gas component unlikely, since not hydrostatically confined and would dissipate very fast
(5*b*) PSPC/two thermals	...	...	$0.48^{+0.12}_{-0.11}$ and 4.6^{+13}_{-2}	$9^{+3.7}_{-2.5}$ and 146^{+47}_{-22}	5.52	...	31.7/29	No excess N_H; hotter gas component unlikely, since not hydrostatically confined and would dissipate very fast

NOTE.—All errors are 1 σ for two interesting parameters and 87% ($\sim 1.5\ \sigma$) for one interesting parameter ($\chi^2 + 2.3$).

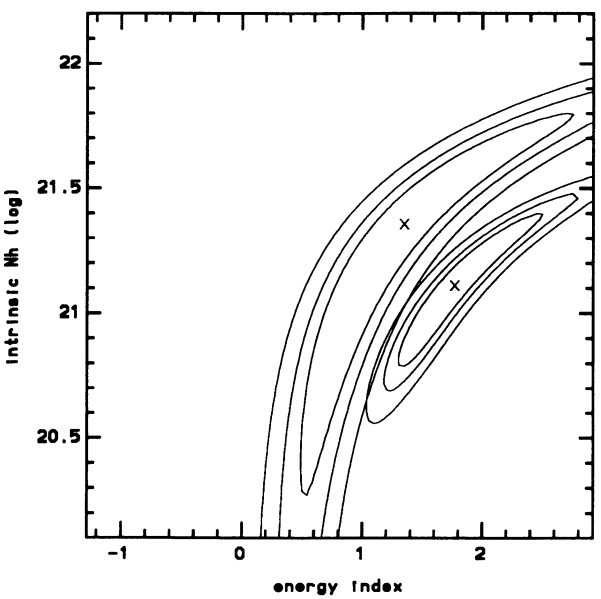

FIG. 7.—The χ^2 contours of Fig. 6 for the PSPC (*to the right*) compared with the same χ^2 contours for a fit to the earlier data from the *Einstein Observatory* IPC (*larger contours, to the left*). The χ^2 contours overlap slightly, but the overlap region is small, suggesting that NGC 6251 showed spectral variations between the PSPC observation and at least one of the two intervals (separated by 2 months) which make up the IPC observation.

Table 5). The required absorption intrinsic to NGC 6251 has dropped by a factor of 3 from the fit to a single power law (becoming marginally consistent with the upper limit of van Gorkom et al. 1989), and the power-law slope is more consistent with that of other elliptical galaxies and BL Lac objects. Since the significance of absorption larger than the Galactic absorption is now less than 3 σ, and the PSPC energy response function remains preliminary (Max-Planck-Institut für Extraterrestrische Physik, Newsletter No. 10, 1992 August), we have also evaluated the parameter values for a power-law and thermal model with no intrinsic absorption (Fig. 8 and entry 4*b* in Table 5). Another acceptable fit ($\chi^2 = 34.6$ with 29 dof, similar to the quality of fit obtained with a power law plus free intrinsic absorption) is obtained: the thermal component has temperature $k_B T_e = 0.49$ keV and distance-normalized volume emission measure (integrated over the entire source)

$$\mathscr{A} \equiv \frac{\int n_e n_p \, dV}{4\pi D_L^2} = 1.0 \times 10^{10} \text{ cm}^{-5} , \qquad (22)$$

and the power-law component has energy index $\alpha_X = 0.27$ and 1 keV flux density $= 3.9 \times 10^{-4}$ keV cm^{-2} s^{-1} keV^{-1} (0.26 μJy). No significant change in χ^2 is obtained if the metal abundance of the thermal gas is varied, and the small metallicity-dependent changes in the best-fit parameters are within our quoted uncertainties.

A second possible two-component model can be produced

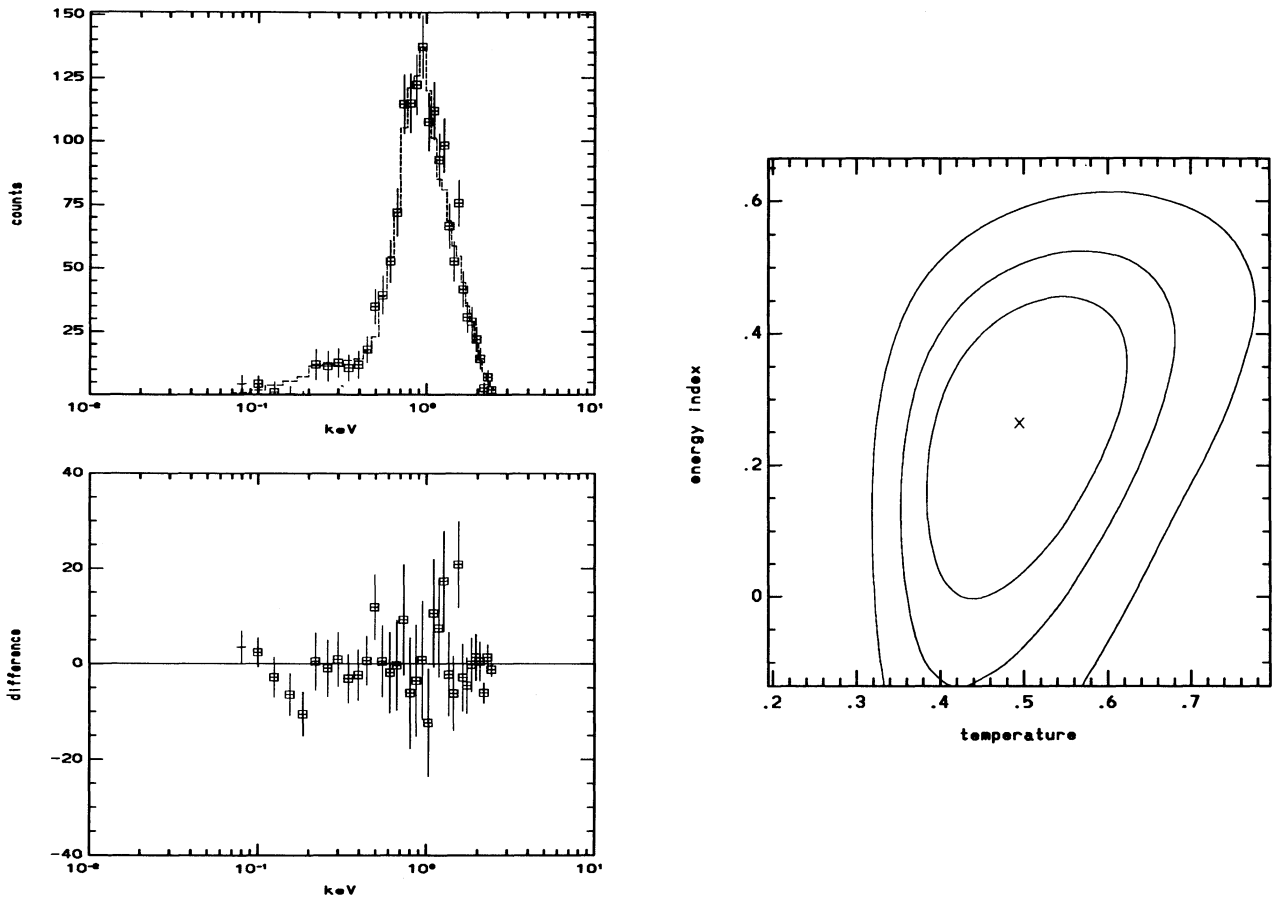

FIG. 8.—Spectral fit of the PSPC data to a model composed of a power-law component and a component from an isothermal gas (with Raymond-Smith thermal emissivity), both absorbed by the (fixed) Galactic gas column and with no absorption intrinsic to NGC 6251 (entry 4*b* in Table 5; cf. Fig. 6). The contour plot is a projection for two of the four free parameters in the model: the energy index for the power-law component and the temperature (in keV) for the isothermal component. The best-fitting spectral index is similar to the radio spectral index of the core at its highest measured frequencies (Jones et al. 1986), supporting an inverse Compton origin for these X-rays. Similar gas temperatures to that found for the thermal component have been measured in some other elliptical galaxies (e.g., Kim et al. 1992).

by replacing the power-law component by a thermal component with a temperature $\geqslant 0.5$ keV. A fit to such a model is also good (entry 5*a* in Table 5), and again the detection of excess absorption is of low significance ($<2\ \sigma$). If a two-component fit without excess absorption is made, the fitted parameters take on the values in entry 5*b* of Table 5. Note that in these two-component fits the hotter component plays approximately the same role as the flat power law does in entries 4*a* and 4*b*, while the parameters of the cool component are little changed.

Thus good fits to the spectrum of NGC 6251 can be made without excess $N_{\rm H}$ using two simple models: (*a*) a flat power law plus thermal emission from a gas at $k_{\rm B}\,T_e \sim 0.5$ keV and (*b*) thermal emission from two gas components, with temperatures $k_{\rm B}\,T_e \sim 0.5$ and 4 keV. Neither thermal component can be identified completely with the extended component of the X-ray source (§ 4; Table 3), since the best-fitting (largest angular size) extended components contribute only a small fraction ($\lesssim 5\%$) of the X-ray flux within the region used for the spectral fits, whereas the 0.5 keV component of the spectral model contributes about 20% of the flux. Thus the appropriate angular size for interpreting these spectral data is the angular size of the unresolved component of the source, as given by equation (19) (or eq. [6]).

Consider first the power-law plus thermal model for the source. If we assume that the gas has cosmic composition, the results of these spectral fits and the structural data imply that the gas has

$$\theta_{cx} < 2\farcs5\,, \quad \mathscr{A} = 1.0 \times 10^{10}\ {\rm cm}^{-5}\,, \quad k_{\rm B}\,T_e = 0.5\ {\rm keV}\,, \tag{23}$$

which imply physical parameters

$$r_{cx} < 1.7\ {\rm kpc}\,, \quad n_{p0} > 0.1\ {\rm cm}^{-3}\,, \quad P_0 > 2 \times 10^{-11}\ {\rm N\ m}^{-2}\,, \quad M_{\rm core} < 6 \times 10^7\ M_\odot \tag{24}$$

for the thermal gas if it is distributed as an isothermal β-model (eq. [3]) with $\beta = \frac{2}{3}$. The quantity $M_{\rm core}$ is the mass of gas contained within radius r_{cx} at the center of the galaxy; the total mass of gas over the entire β-model distribution is not a meaningful quantity, as explained in § 4. Note that the β-model leads to a lower central gas density than would a uniform-sphere model for the core gas; because it is has a range of densities, it is a more efficient X-ray–emitter for the same mass of gas. The central gas pressure, P_0, is insufficient to confine the jet in the VLBI core of NGC 6251, which requires a central pressure $P_0 > 5 \times 10^{-8}$ N m^{-2} (Jones et al. 1986), unless the

gas is confined in a region of radius $\lesssim 10$ pc and has a correspondingly higher central density than in equation (24).

We can ask whether the thermal gas of equation (23) will be stable in the center of the galaxy. The cooling time of the gas is

$$\tau_{\rm cool} = 30 \times 10^6 (n_p/{\rm cm}^{-3})^{-1} (k_{\rm B}\, T_e/{\rm keV})^{1/2}\ {\rm yr} \qquad (25)$$

(eq. [5.23] of Sarazin 1986), which for these gas parameters corresponds to $\lesssim 180 \times 10^6$ yr. This cooling time is much less than a Hubble time (although it is several central dynamical times, or sound crossing times, in the galaxy), so that the gas either is falling toward the center of the galaxy in a cooling flow or is being dynamically maintained by a supply of energy from the core (e.g., by radiative heating or by the jet's momentum deposition) *if it has been held in this configuration in the core for many cooling times.* An alternative possibility is that the presence of this core gas is a *recent* phenomenon, and that it has been in the core only for a relatively short time. The interesting coincidence between the central cooling time of the gas and the radio source lifetime that can be estimated from the source size and the 8000 km s^{-1} jet velocity suggested by Perley et al. (1984a) may argue in favor of this latter interpretation. The identification of this gas as a cooling flow also suggests that it represents the central, cooling part of the large-scale atmosphere suggested by the structural fits (§ 4).

Turning now to the spectral fit in terms of two thermal components, we find that the inferred core radius, proton density, and gas mass in the cooler component are not significantly different from their results above (eqs. [23] and [24]), since the distance-weighted volume emission measure and temperature are similar to those in the power-law plus thermal model. For the hotter thermal component the structural and spectral fits indicate

$$\theta_{cx} < 2\farcs5\,,\quad \mathscr{A} = 1.5 \times 10^{11}\ {\rm cm}^{-5}\,,\quad k_{\rm B}\, T_e = 4.6\ {\rm keV}\,, \qquad (26)$$

which lead to physical parameters

$$r_{cx} < 1.7\ {\rm kpc}\,,\quad n_{p0} > 0.5\ {\rm cm}^{-3}\,,$$
$$P_0 > 8 \times 10^{-10}\ {\rm N\ m}^{-2}\,,\quad M_{\rm core} < 2 \times 10^8\ M_\odot \qquad (27)$$

if this gas is distributed as an isothermal β-model (eq. [3]) with $\beta = \frac{2}{3}$. This component of the gas has a substantially higher pressure than the cooler component (eq. [24]), unless the cool component has a small filling factor in the core of NGC 6251, but still has insufficient pressure to confine the VLBI jet unless it is contained in a region with $r_{cx} \lesssim 100$ pc. At its most diffuse (eq. [27]), the hotter component has a cooling time that is comparable to that of the cool component of the gas.

Which of these two composite models for NGC 6251 is to be preferred? The thermal plus power-law model has the advantage of representing both the presence of a nonthermal source (with the same X-ray spectral index as the radio spectral index, and hence with a plausible origin in inverse Compton emission; § 5.3) and of a gaseous halo of the type that might be found in other elliptical galaxies. The two–thermal-component model, on the other hand, might represent the central part of a cooling flow from a large-scale, low-density, halo of NGC 6251 (or from the entire group of galaxies of which it is a member), which has undergone a partial condensation into cooler and hotter components. However, the hotter component of the gas is very difficult to confine in either NGC 6251 or the NGC 6251 group of galaxies (see § 4) and must be a transient phenomenon. The interpretation of the two-thermal component model of the spectrum as a cooling flow is therefore unlikely, and since no other source for the hot component of the gas is evident, we tentatively select the power-law plus thermal model as the more plausible model for the spectrum and structure of the core X-ray source.

5.3. *The Nonthermal Component in the Core Source*

Having determined that a mixture of nonthermal and thermal emission is the most plausible model for the X-ray emission of the core, and the properties of the thermal component are reasonable, it remains for us to examine whether or not the parameters of the nonthermal component are also reasonable.

The spectral index of the nonthermal component is somewhat uncertain. Without allowing excess absorption, we find a best-fit index of 0.27 (Fig. 8 and entry 4*b* in Table 5), but if some as yet undetected absorbing gas is present the best fit becomes 1.0 and values as large as 1.6 are allowed (entry 4*a* in Table 5). We have little with which to compare our results. Although it is thought likely that radio galaxies emit nonthermal X-ray radiation (e.g., Fabbiano et al. 1984), detections have been weak and spectral indices are unknown, except for Cen A, where the energy index varies between about 0.6 and 0.9 (Feigelson et al. 1981). However, recent ideas concerning "unification" of classes of radio sources, in which relativistic jets are assumed to be viewed at different line-of-sight angles, relate low-luminosity FR 1 (Fanaroff-Riley Class 1; Fanaroff & Riley 1974) radio galaxies with BL Lac objects (e.g., Browne 1989). NGC 6251 can be classified as an FR 1 radio galaxy on the basis of its luminosity and morphology (which lacks radio hot spots). Spectral indices have been measured for many BL Lac objects. A sample of 24 radio-selected ones observed with the *Einstein Observatory* IPC gives a mean index of 1.0 (at 0.2–3.5 keV) with remarkably small uncertainty, and is consistent with zero dispersion (Worrall & Wilkes 1990). The X-ray spectrum of NGC 6251 may be consistent with this BL Lac object range, if we assume some excess absorption. However a spectral index as flat as 0.27 is also not remarkable when taking into account Worall & Wilkes's (1990) finding that X-ray–selected BL Lac objects, thought to be intermediate in orientation between radio-selected BL Lac objects and FR 1 radio galaxies (e.g., Padovani & Urry 1990), show finite dispersion in spectral index. Furthermore, spectral flattening to lower energies has been reported for the 0.1–10 keV spectra of BL Lac objects (Madejski 1985; Barr et al. 1989; Madejski & Schwartz 1989), and the PSPC's energy band is lower than, although overlapping, that of the IPC.

Jones et al. (1986) model their VLBI radio data for NGC 6251 into a core and jet. They find that the core turns over at 13.5 GHz, a higher frequency than for the jet, where it represents about 80% of the total VLBI emission. The spectral index above the turnover is given as 0.25, in excellent agreement with the X-ray index without excess absorption. This suggests a direct relationship between the X-ray and radio emission through the synchrotron self-Compton process. When the equations formulated by Marscher (1983) for spherical symmetry are applied, we find that strong bulk relativistic motion of the core is not required. Our limit to the bulk relativistic Doppler factor is $\delta \gtrsim 1$, where the limit derives from having only an upper limit to the angular size of the radio core of 0.2 mas. Although Doppler factors derived in such a way are notoriously uncertain owing to the high powers of the radio parameters which enter the equations, at least our limit enables us to check for self-consistency with other, independent evidence for relativistic motion.

There are two pieces of evidence suggesting relativistic motion in the VLBI jet. The first is from Jones et al. (1986), who interpret the measured VLBI jet-to-counterjet ratio using a twin-jet model, where relativistic effects enhance the brightness of the jet traveling mostly toward the observer relative to the oppositely directed jet, to set limits on the velocity of the jet, v, and its angle relative to the line of sight, i:

$$\frac{v}{c}\cos i > 0.7 . \tag{28}$$

The second piece of evidence (Jones 1986) is due to a "blob" in the VLBI jet remaining stationary between the observations of 1983 March and 1985 April, from which

$$\frac{v \sin i}{c - v \cos i} < 0.4 . \tag{29}$$

Figure 9 is similar to a figure in Jones (1986) showing these two constraints. The second (labeled v_T) is the most restrictive in that it requires $i < 10°$ and makes what is already a long VLA jet ($\sim$200 kpc for $H_0 = 50$ km s^{-1} Mpc^{-1}) even longer when projected onto the plane of the sky. Contours of δ are shown on the figure. Our first conclusion is that our result $\delta \gtrsim 1$ *does not require* the constraint $i < 10°$.

Jones (1986) was uneasy with the large source size implied by the strong constraint on i, and suggested that rather than twin relativistic jets, the jet changes direction on time scales comparable to those required to fuel the lobes—the so called "flip-flop" model. Birkinshaw et al. (1993) have mapped the source at low frequency (330 MHz) to search for steep-spectrum features indicative of aged electrons on the counterjet side of the source but have failed to find any. We therefore favor an interpretation in which the jet is twin-beamed but where the stationary feature in the VLBI jet is not indicative of the bulk flow, or where the intrinsic jet direction varies by $\gtrsim 10°$ between the VLBI and VLA scales.

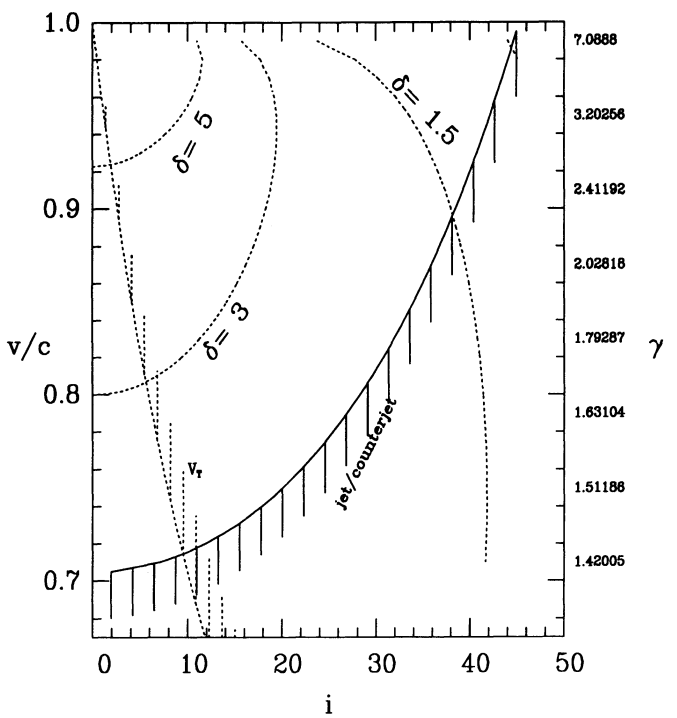

FIG. 9.—Limits to the speed and inclination of the parsec-scale radio jet in the core of NGC 6251 based on the radio jet/counterjet ratio and the limit to the transverse velocity (v_T) of a bright knot in the VLBI radio source, after Jones (1986). Contours of constant bulk relativistic Doppler factor δ are also shown. Our conclusion that $\delta \gtrsim 1$, based on the assumption that the power-law component of the core source is produced by inverse Compton radiation, *does not require* the strong constraint of $i < 10°$ which would make NGC 6251 exceptionally large. We infer instead that the stationary feature in the VLBI jet is not indicative of the bulk flow, so that the v_T limit in the figure is not applicable. An inclination for the jet of $i \sim 25°$ is suggested from fitting our X-ray observations to the beaming model of Padovani & Urry (1990).

We can infer an angle to the line of sight for the jet of NGC 6251 by placing the object in the framework of the unified model for BL Lac objects and FR 1 radio galaxies. This model assumes two emission components; one is beamed and dominates when a jet is near to the line of sight, and the other is unbeamed and dominates when the twin jets lie in the plane of the sky. For NGC 6251 we are in the rare position for X-ray measurements of having separated thermal (unbeamed) emission and nonthermal (beamed) emission. Padovani & Urry (1990) parameterized the total luminosity L in terms of unbeamed luminosity L_u and beamed luminosity $L_{\rm jet}$, as

$$\begin{aligned} L &= L_u + L_{\rm jet} \\ &= L_u + f\delta^4 L_u , \end{aligned} \tag{30}$$

where f is the fraction of the unbeamed luminosity in the jet. They treat the statistics (luminosity functions) of X-ray–selected BL Lac objects compared with radio-selected FR 1 galaxies and find best-fit parameters

$$\gamma_x = 3.4 , \quad i_c = 31° , \quad f = 0.14 , \tag{31}$$

where γ_x is the Lorentz factor and i_c is the critical angle between a source being jet-dominated and being dominated by the unbeamed radiation (i.e., the angle where $L_u = L_{\rm jet}$). The PSPC data (0.2–2.5 keV) for NGC 6251 give luminosities of 8.5×10^{34} W in the thermal (presumably unbeamed) component, and 3.2×10^{35} W in the power-law (beamed) component, for no excess absorption. Using the ratio,

$$L_{x,\rm jet} = 3.8 \times L_{x,u} , \tag{32}$$

that this implies, with equations (30) and (31), leads to

$$i = 25° , \quad \delta \sim 2 . \tag{33}$$

The results depend, but not strongly, on our assumption concerning intrinsic absorption. Luminosities computed from the model with excess absorption (entry 4*a* in Table 5) imply $i = 21°, \delta \sim 3$.

The values derived for i and δ fit in well with the constraint from the jet-to-counterjet ratio (see Fig. 9) and the value of δ from the synchrotron–self-Compton calculation. We further infer that as long as the source size is close to the VLBI upper limit of 0.2 mas, all the nonthermal X-ray radiation could be Compton emission. It is of particular note that NGC 6251 fits into the unified model assuming that the thermal emission we have separated spectrally from the core radiation is the required unbeamed component. It will be of interest to search for such a thermal X-ray component in other FR 1 radio galaxies.

6. CONCLUSIONS: A MODEL FOR THE SOURCE

From our *ROSAT* PSPC image and spectrum of NGC 6251 we can conclude the following:

1. The X-ray emissivity of the radio jet of NGC 6251 is at least an order of magnitude less than that of M87 per unit

radio luminosity, and the overall spectrum of feature A in the jet of NGC 6251 is consistent with synchrotron emission from a power-law distribution of electrons cut off above an energy $\approx 10^{12}$ eV.

2. The atmosphere of NGC 6251, which accounts for $\sim 10\%$ of the total X-ray flux, cannot provide sufficient static pressure to confine the VLA-scale radio jet, but could supply the electron density needed to explain the Faraday rotation properties of the jet described by Perley et al. (1984a).

3. The nuclear X-ray source, which accounts for $\sim 90\%$ of the total X-ray flux, is unresolved in these observations and hence has FWHM $\lesssim 3$ kpc (adopting the model-dependent estimate of eq. [7]).

4. The X-ray spectrum of the galaxy can be interpreted either in terms of excess neutral hydrogen absorption and a simple steep power law (with energy index $\alpha_X \approx 1.8$) or in terms of a composite spectrum with a low-temperature thermal component and either a power-law component or a high-temperature thermal component, and little or no excess neutral hydrogen absorption. Since no site for the (large) excess $N_H \approx 1.3 \times 10^{21}$ cm^{-2} has been found, and since a high-temperature thermal gas cannot be in hydrostatic equilibrium in the galaxy, it appears that the model in terms of power-law plus 0.5 keV thermal components is to be preferred. The 0.5 keV central gas may represent the inner, cooling-flow part of the large-scale component of the source identified from the radial profile.

5. The power-law component is consistent with synchrotron–self-Compton emission from the VLBI core with a bulk relativistic Doppler factor $\delta \gtrsim 1$. Our decomposition of the X-ray core into beamed (nonthermal) and unbeamed (thermal) emission fits Padovani & Urry's (1990) model unification scheme that relates BL Lac objects and radio galaxies, implies that NGC 6251's VLBI jet lies at $\sim 25°$ to the line of sight, and suggests that the type of thermal emission we find in NGC 6251 may be common in low-luminosity radio galaxies.

An interesting synthesis from these conclusions is a possible model for the processes in the core of NGC 6251. If the spectrum is interpreted in terms of a power-law component plus 0.5 keV gas emission, then the 0.5 keV gas is thermally unstable and must be participating in a cooling flow (unless this flow is halted by heating, perhaps regulated by a feedback mechanism). In this case, equations (24) and (25) show that about $M_{\rm core}/\tau_{\rm cool,core} = 0.3\ M_\odot\ {\rm yr}^{-1}$ of gas is falling toward the nucleus (note that this estimate is independent of the unknown angular size of the X-ray–emitting region). This is an interesting rate of mass infall; it is the typical inward mass flux required to fuel a medium-power AGN. Thus a consistent model for the source can be suggested in which the thermal gas drifts into the center of the galaxy as it radiates energy (principally at X-ray wavelengths), and this mass infall is powering the AGN, which then radiates the power-law component of the energy. This same type of model has been used by (e.g.) Fabbiano, Gioia, & Trinchieri (1989) to explain correlations between the radio and X-ray core luminosities of elliptical galaxies.

The nonthermal component of NGC 6251 has a luminosity of 3.2×10^{35} W (in 0.2–2.5 keV; the total luminosity may be a factor of a few larger). The inward cooling mass flux of $0.3\ M_\odot\ {\rm yr}^{-1}$ can produce this luminosity if it is converted to energy with an efficiency $\approx 2 \times 10^{-4}$. The Eddington luminosity for an accretion-powered source is

$$L_{\rm E} = \frac{4\pi GMc}{\kappa_e} \approx 1.3 \times 10^{31} \left(\frac{M}{M_\odot}\right) {\rm W}\ , \qquad (34)$$

where κ_e is the electron opacity and M is the mass of the central object. Thus, if the X-radiation is produced by sub-Eddington accretion, then the mass of the central black hole must exceed $2 \times 10^4\ M_\odot$ and could be as large as the masses required in typical AGNs, or as large as the mass suggested for a central black hole in NGC 6251 by Young et al. (1979).

For this picture to be consistent, the cooling lifetime of the gas must be comparable to the lifetime of the radio source and central core source. The cooling time of the 0.5 keV gas is $\tau_{\rm cool} \approx 2 \times 10^8$ yr (eq. [25]), and the lifetime of the radio source may be estimated from the 8000 km s^{-1} jet velocity suggested by Perley et al. (1984a) and the 1 Mpc half-size of the radio source to be $\tau_{\rm source} \approx 1.2 \times 10^8$ yr. These lifetimes are in adequate agreement given the crudeness of the model estimates.

Further tests of this model can be suggested. It is important to conduct better searches for the H I (or H_2) that might absorb the X-radiation, through further observations of NGC 6251; emission- and absorption-line studies in the 21 cm line and emission studies in the 3 mm CO line are indicated. Higher resolution X-ray data might achieve a structural separation between the nuclear components that we have only been able to distinguish in the spectrum. Deeper X-ray studies with a less extended PRF will obtain better information on the atmosphere of the galaxy, and should be able to make stronger statements about the pressure provided by this gas near the jet of NGC 6251 and set better limits to the possible contribution of any atmosphere of the NGC 6251 group of galaxies. The NGC 6251 group needs better optical studies also, to determine group membership and to decide what confining mass there is that might hold a group atmosphere. Finally, further optical studies of the emission from the jet are needed to decide whether the emission is synchrotron emission from electrons in the jet (as assumed in § 4) or arises from a chance superposition of a foreground (or background) galaxy, and to show that the emission is continuum and not largely made up by line emission from a star-forming region (like Minkowski's object; van Breugel et al. 1985).

This research was supported by NASA grants NAG5-1648 and NAG5-1724, and NASA contract NAS5-30934. We thank Harvey Tananbaum for comments on a preliminary form of this paper.

REFERENCES

Aschenbach, B. 1991, Rev. Mod. Astron., 4, 173
Barr, P., Giommi, P., Pollock, A., Tagliaferri, G., Maccagni, D., & Garilli, B. 1989, in IAU Symp. 134, Active Galactic Nuclei, ed. D. E. Osterbrock & J. Miller (Dordrecht: Kluwer), 191
Begelman, M. C., Blandford, R. D., & Rees, M. J. 1980, Nature, 287, 307
Biretta, J. A., Stern, C. P., & Harris, D. E. 1991, AJ, 101, 1632
Birkinshaw, M., Zheng, X. W., Ho, P. T. P., & Reid, M. J. 1993, in preparation
Browne, I. W. A. 1989, in BL Lac Objects, ed. L. Maraschi, T. Maccacaro, & M.-H. Ulrich (Berlin: Springer-Verlag), 401
Cavaliere, A., & Fusco-Femiano, R. 1978, A&A, 70, 677
Cohen, M. H., & Readhead, A. C. S. 1979, ApJ, 233, L101
Fabbiano, G., Gioia, I. M., & Trinchieri, G. 1989, ApJ, 347, 127
Fabbiano, G., Miller, L., Trinchieri, G., Longair, M., & Elvis, M. 1984, ApJ, 277, 115

Fanaroff, B. L., & Riley, J. M. 1974, MNRAS, 167, 31P
Feigelson, E. D., Schreier, E. J., Delvaille, J. P., Giacconi, R., Grindlay, J. E., & Lightman, A. P. 1981, ApJ, 251, 31
Forman, W., Jones, C., & Tucker, W. 1985, ApJ, 293, 102
Gruber, R. 1992, in Data Analysis in Astronomy IV, ed. V. Di Gesu et al. (New York: Plenum), 153
Hardee, P. E., White, R. E., Norman, M. L., Cooper, M. A., & Clarke, D. A. 1992, ApJ, 387, 460
Hasinger, G., Turner, T. J., George, I. M., & Boese, G. 1992, NASA/GSFC Office of Guest Investigator Programs, Calibration Memo CAL/ROS/92-001
Heckman, T. M., Carty, T. J., & Bothun, G. D. 1985, ApJ, 288, 122
Henriksen, R. N., Bridle, A. H., & Chan, K, L. 1982, ApJ, 257, 63
Henriksen, R. N., Vallée, J. P., & Bridle, A. H. 1981, ApJ, 249, 40
Jones, D. L. 1986, ApJ, 309, L5
Jones, D. L., et al. 1986, ApJ, 305, 684
Keel, W. C. 1988, ApJ, 329, 532
Kim, D.-W., Fabbiano, G., & Trinchieri, G. 1992, ApJS, 80, 645
Leahy, J. P. 1984, MNRAS, 208, 323
Loken, C., Burns, J. O., Clarke, D. A., & Norman, M. L. 1992, ApJ, 392, 54
Madejski, G. M. 1985, Ph.D. thesis, Harvard Univ.
Madejski, G. M., & Schwartz, D. A. 1989, in BL Lac Objects, ed. L. Maraschi, T. Maccacaro, & M.-H. Ulrich (Berlin: Springer-Verlag), 267
Marscher, A. P. 1983, ApJ, 264, 296
Miller, L., Longair, M. S., Fabbiano, G., Trinchieri, G., & Elvis, M. 1985, MNRAS, 215, 799
National Radio Astronomy Observatory 1990, VLA Calibrator Book (Socorro: NRAO)
Nieto, J. C., Coupinot, G., LeLievre, G., & Madsen, C. 1983, MNRAS, 203, 39P
Owen, F. N., Hardee, P. E., & Cornwell, T. J. 1989, ApJ, 340, 698
Padovani, P., & Urry, C. M. 1990, ApJ, 356, 75
Perley, R. A., Bridle, A. H., & Willis, A. G. 1984a, ApJS, 54, 291
Perley, R. A., Dreher, J. W., & Cowan, J. 1984b, ApJ, 285, L35
Pfefferman, E., et al. 1987, in Soft X-Ray Optics and Technology, ed. E.-E. Koch & G. Schmahl, (Proc. SPIE, Vol. 733), 519
Prestage, R. M., & Peacock, J. A. 1988, MNRAS, 230, 131
Raymond, J. C., & Smith, B. W. 1977, ApJS, 35, 419
Sarazin, C. L. 1986, Rev. Mod. Phys., 58, 1
Schneider, S. E., Helou, G., Salpeter, E. E., & Terzian, Y. 1983, ApJ, 273, L1
Stark, A. A., Gammie, C. F., Wilson, R. W., Bally, J., Linke, R. A., Heiles, C., & Hurwitz, M. 1992, ApJS, 79, 77
Tody, D. 1986, in Instrumentation in Astronomy VI, ed. D. L. Crawford (Proc. SPIE, Vol. 627), 733
Trümper, J. 1983, Adv. Space Res., 2, 241
———. 1992, QJRAS, 33, 165
van Breugel, W., Filippenko, A. V., Heckman, T., & Miley, G. 1985, ApJ, 293, 83
van Gorkom, J. H., Knapp, G. R., Ekers, R. D., Ekers, D. D., Laing, R. A., & Polk, K. S. 1989, AJ, 97, 708
Waggett, P. C., Warner, P. J., & Baldwin, J. E. 1977, MNRAS, 181, 465
Willis, A. G., Strom, R. G., Perley, R. A., & Bridle, A. H. 1982, in IAU Symp. 97, Extragalactic Radio Sources, ed. D. S. Heeschen & C. M. Wade (Dordrecht: Reidel), 141
Worrall, D. M., et al. 1992, in Data Analysis in Astronomy IV, ed. V. Di Gesu et al. (New York: Plenum), 145
Worrall, D. M., & Wilkes, B. J. 1990, ApJ, 360, 396
Young, P. J., Sargent, W. L. W., Kristian, J., & Westphal, J. A. 1979, ApJ, 234, 76